2017-08-04

Simulation-Optimization Approaches for Demand Side Management in Smart Grids

Mehrad Bastani
University of Miami, m.bastani@umiami.edu

UNIVERSITY OF MIAMI

SIMULATION-OPTIMIZATION APPROACHES FOR DEMAND SIDE MANAGEMENT IN SMART GRIDS

By

Mehrad Bastani

A DISSERTATION

Submitted to the Faculty
of the University of Miami
in partial fulfillment of the requirements for
the degree of Doctor of Philosophy

Coral Gables, Florida

August 2017

UNIVERSITY OF MIAMI

A dissertation submitted in partial fulfillment of
the requirements for the degree of
Doctor of Philosophy

SIMULATION-OPTIMIZATION APPROACHES FOR DEMAND SIDE MANAGEMENT IN SMART GRIDS

Mehrad Bastani

Approved:

_____ Nurcin Celik, Ph.D. Associate Professor of Industrial Engineering	_____ Shihab Asfour, Ph.D. Professor and Associate Dean of College of Engineering
_____ Murat Erkoc, Ph.D. Associate Professor of Industrial Engineering	_____ Seok G. Lee, Ph.D. Assistant Professor of Industrial Engineering
_____ Hungtan Liu, Ph.D. Professor of Mechanical and Aerospace Engineering	_____ Guillermo Prado, Ph.D. Dean of the Graduate School

BASTANI, MEHRAD (Ph.D., Industrial Engineering)
(August 2017)

Simulation-optimization Approaches for Demand Side Management in Smart Grids

Abstract of dissertation at the University of Miami

Dissertation supervised by Professor Nurcin Celik
No. of pages in text. (92)

In smart and connected communities (S&CCs), energy, transportation, water, public safety, and all other services need to be managed efficiently to support smooth operation while providing a clean, economical, and safe environment for citizens. The power system infrastructure is the most important part of S&CCs that affects the functionality of all components. Over the past two decades, power systems have witnessed significant changes in the use of renewable and distributed energy resources, energy control technologies, and technical advances in communication and computation, which has led to the development of smart grids. Smart grids provide sustainable power grids with the capabilities of self-healing and automatic execution in an isolated mode, but the operation and control planning of smart grids are challenging procedures. The main challenges arise from energy load scheduling of customers using interruption load management (ILM) and load shifting strategies; communication between customers and utility companies or third-party aggregators to increase customer satisfaction and decrease costs; and the need to provide reliable and high-quality energy to customers. In this doctoral study, novel simulation and optimization approaches for demand side management (DSM) in smart grids are introduced to address the main challenges in the operation and control planning of smart grids. To this end, this study investigates efficient DSM programs for smart grids and addresses the primary challenges in two broad frameworks: (1) a deterministic optimization framework

for load shifting in smart grids, which can obtain optimal scheduling for time-shiftable energy loads using an advanced ϵ-constraint optimization method, and (2) a stochastic and dynamic simulation optimization framework for DSM programs in smart grids that finds near-optimal solutions for ILM with uncertain loads. These two frameworks provide a simulation and optimization tool for utility companies or third-party aggregators to provide day-ahead energy load scheduling based on desirable DSM strategies. The proposed frameworks are applied in two synthetic smart grid case studies. The results of the case studies show that the proposed frameworks are able to meet the desired energy load curves while resulting in better objective functions. This doctoral research reveals that both deterministic and stochastic DSM programs are promising tools to optimize and boost the implementation of DSM programs and attain several benefits.

ACKNOWLEDGEMENTS

First of all, I would like to express my sincerest gratitude to my advisor, Dr. Nurcin Celik, for her constant support and encouragement throughout the completion of my doctoral degree. She has guided me in my research and career and has provided me with tremendous support in every aspect of my graduate life, for which I will always be grateful. I would also like to thank my committee members, Dr. Shihab Asfour, Dr. Murat Erkoc, Dr. Seok G. Lee, and Dr. Hongtan Liu, for their invaluable input on my doctoral research. Their rigorous attitudes toward science, words of encouragement, and fair-minded assessment of this work have inspired me to strive to do my best. I would also like to state my appreciation to the faculty and staff at the University of Miami, who have significantly helped me along this path. Moreover, thanks to all members in our Simulation and Optimization Research Lab (SimLab): Haluk Damgacioglu, Aristotelis Thanos, Xiaoran Shi, Talal Mohammadghazali Alyamani, Duygu Yasar, Greg Collins, Danielle Coogan, and Delante E. Moore. I have been greatly influenced by their great passion in research and pursuit of new knowledge. I will always remember my experience cooperating with them and will always cherish our friendship.

Finally, I cannot express enough thanks to my father, Shahrokh, my mother, Gohar, my sister, Sepideh, and my brother, Maziar, for helping me through the hard times.

Table of Contents

List of Figures

Page

List of Tables

Page

Chapter 1

Introduction

In future smart and connected communities (S&CCs), energy, transportation, water, public safety, and all other services should be managed to support smooth operation while providing a clean, economic, and safe environment for citizens. Electricity is the most versatile and widely used form of energy, and global demand for it is continuously growing. Smart grids can improve the reliability of electricity services for customers in future smart cities by identifying and resolving faults on the power grid, better managing voltage, and self-healing. A smart grid is an evolved energy grid system that manages electricity in a sustainable, resilient, and economic manner, built on an advanced cluster of distributed generation units, renewable energies, energy storage, equipment, and circuits for generating, transmitting, transforming, and distributing energy. Although smart grids provide several advantages over traditional power grids, smart cities rely heavily on a reliable flow of electricity, and power outage is still a major challenge. New types of energy loads such as plug-in hybrid electric vehicles (PHEVs), which can potentially double residential customer consumption, have especially caused energy providers to need reliable and flawless energy supply planning. In power networks that include smart grids, the total power supplied from traditional and renewable energy sources must be greater or equal to customer demand. However, there are times when power generation may not sufficiently satisfy demand, which can be significantly higher than its predicted value. During these times, the power network is at risk due to severe voltage oscillations that may cause minor or major (even permanent) failures. To prevent such failures, utilities commonly plan for their total installed electricity generation capacity to satisfy the forecasted peak demand,

considering a margin of error. Most power systems are also supported by contingency energy sources in an idle state in the grid but ready to be used in case of power outages. These systems are typically managed in a way such that demand is satisfied at a minimum possible cost with the least expensive generation sources being utilized first, followed by other more expensive sources. In order to increase reliability in smart grids and decrease blackout and brownout periods, demand side management (DSM) is used to control and reduce peak demand. Demand side management programs are mainly used to avoid potential instabilities in power networks, providing economic benefits by utilizing only the least-expensive sources of generation and eliminating the need for constructing additional power plants to satisfy increasing peak demand [1-5]. Demand side management has become a significant function in energy management due to its potential to reduce the cost of peak demand satisfaction [6-8]. In energy management literature, there are six main groups of DSM: 1) peak clipping, which reduces peak load demand by using time-based incentives for interrupted customers; (2) load shifting, which shifts loads from on-peak to off-peak time periods; (3) valley filling, which shifts peak demand usage to low demand periods, but the term can refer to any program or strategy aimed at filling the usage valley between peak uasage times; (4) flexible load shape, which provides control over customers during critical periods in exchange for various incentives; (5) strategic conservation, which reduces energy demands directly on customers' premises; and (6) strategic load building (load growth), which optimizes daily response in case of large demand [1-9]. Load shifting and peak clipping, also known as interruption load management (ILM), are the most popular DSM programs due to their ease of application and efficiency. This doctoral dissertation investigates the effectiveness of DSM programs, including load shifting and

ILM, on future smart grids using two main frameworks: F1) a deterministic optimization framework for DSM programs in smart grids and F2) a stochastic and dynamic simulation optimization framework for DSM programs in smart grids. Details and contributions of the proposed frameworks are provided in the following subsections.

1.1. A Deterministic Multi-Objective Optimization Framework for DSM in Smart Grids (F1)

Increasing populations, growing electrical energy consumption, and the integration of renewable energy sources into electricity grids over the last few decades has made maintaining grid power balance a major challenge for energy providers [10]. Due to the deployment of renewable energies and the need for high reliability, traditional power grids will move toward becoming intelligent modern power grids known as smart grids in the near future [11]. Smart grids play a critical role in transforming the traditional power grid system into one that provides a user-oriented service and guarantees high security, quality, and economic efficiency. However, to maintain sustainability in smart grids, the total capacity of installed generation in the system must be larger than the maximum load demand to ensure the security of supply in the face of uncertainty (e.g. generation breakdowns and interruptions to primary fuel sources) and variations in energy supply due to adverse weather [9]. DSM programs have been proposed as a major dimension of future power supply and control to prevent blackouts and brownouts during load variation and uncertain energy generation. DSM programs are typically a set of programs that harmonize the activities of energy providers and consumers to control energy consumption. These programs monitor and influence load profiles during peak load demand and are used to avoid installing new generation infrastructure.

Despite the progress achieved in the field of DSM, a simultaneous consideration of cost minimization and customer satisfaction maximization has not yet been addressed. The proposed deterministic multi-objective optimization framework for DSM in this dissertation attempts to minimize cost and greenhouse gas (GHG) emissions while maximizing customer satisfaction. Fig. 1 represents the proposed mixed-integer multi-objective optimization framework for implementing load shifting and ILM programs in smart grids to satisfy desired demand.

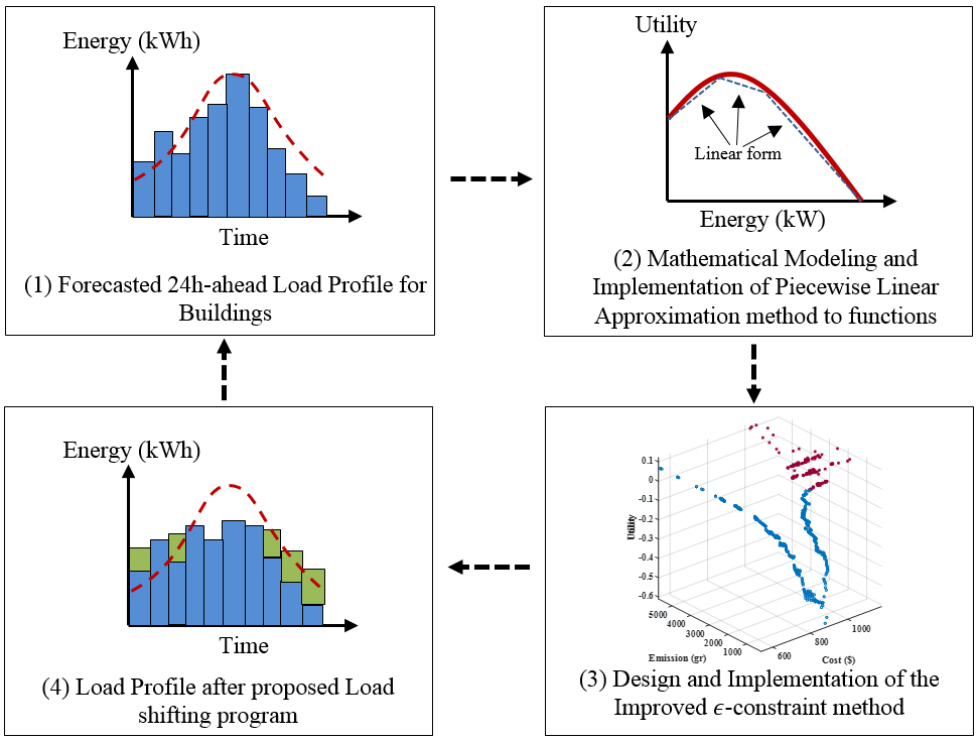

Fig. 1: Proposed multi-objective optimization DSM framework

The proposed framework includes four main components: (1) a forecasting model that creates a 24-hour-ahead load profile using historical data about renewable energy sources in smart grids, (2) a mathematical model of the load shifting and ILM problem and implementation of a piecewise linear approximation method to achieve the mixed-integer multi-objective optimization model, (3) an advanced ϵ-constraint model for the mixed-

integer multi-objective optimization problem that acquires Pareto frontier solutions with a higher number of non-dominated solutions and less computational time, and (4) mathematical scheduling for load profile construction based on the results of the framework. This proposed framework is implemented for a small case study of smart grids for efficiency and effectiveness purposes.

1.2. A Stochastic and Dynamic Simulation Optimization Framework for DSM in Smart Grids with Uncertain Loads (F2)

Implementation of DSM programs have been heavily studied in context of deterministic device loads; however, less attention has been paid to variations in device loads. The consideration of load variation can affect all DSM strategies to produce solutions that might violate the required energy curtailment (infeasible solutions) [3, 12]. The assumption of constant energy consumption is critical for DSM programs' practicality and realism, but as in the real world, the hourly energy load consumption of electrical devices can be altered by several factors (e.g. a device's selected program; different modes such as on, off, and standby; etc.). This portion of this doctoral research is novel in its consideration of device load variation in the ILM problem, and variation in device load is incorporated as an additive variation factor and addressed via the conduct of extensive simulation experiments to generate loads, considering the normal load distribution for each device. To illustrate this, imagine a device with a base load x that ranges from $x - 1$ to $x + 1$. A traditional deterministic DSM strategy may generate a solution that does not interrupt this device in a specific time period assuming that its load is x. Further, assume that in this time period, when applying the deterministic solution, the total demand is exactly equal to the desired power generation. In the case that this device's load becomes

$x + 1$ then the solution automatically becomes infeasible. The proposed evolutionary simulation optimization framework for ILM is composed of three major components: 1) a genetic algorithm that progressively discovers new solutions for the scheduling of interruptible loads, 2) a simulation model that acquires the performance of different interruption scenarios, and 3) a complete ranking optimal computing budget allocation (OCBA) that optimizes the allocation of the number of replications dedicated to each simulation scenario and identifies the top m-best solutions for the genetic algorithm (Fig. 2).

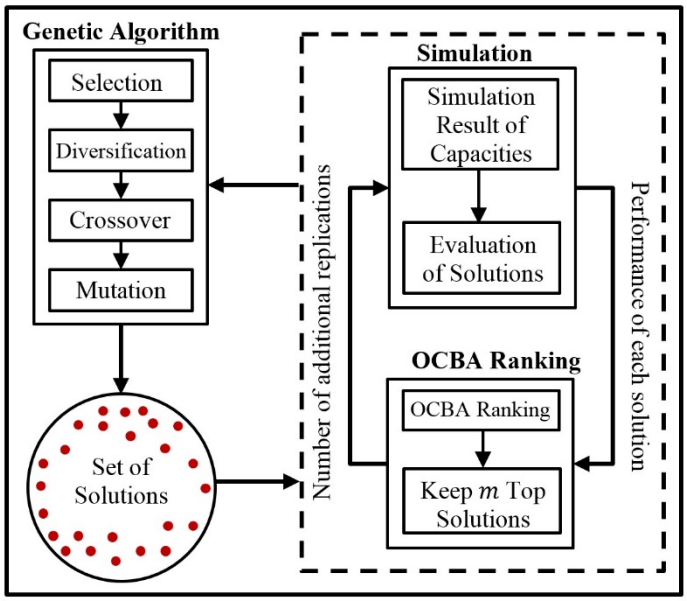

Fig. 2: Proposed simulation optimization framework for ILM

1.3. Summary of Proposed Contributions

The main contributions of this research may be categorized as the contributions of the deterministic multi-objective optimization framework for DSM in smart grids (F1) and the contributions of the stochastic and dynamic simulation optimization framework for DSM in smart grids with uncertain loads (F2). These contributions are summarized below:

- *F1-Contribution 1:* This framework is the first to simultaneously consider cost minimization, emission minimization, and customer satisfaction for a load shifting strategy. Furthermore, the proposed framework is converted to mixed-integer linear programming (MILP) for higher accuracy and lower computational time.
- *F1*-Contribution 2: This study develops a novel multi-objective optimization method to more efficiently find a Pareto frontier solution set. The proposed methodology, "advanced ϵ-constraint multi-objective optimization," has the ability to obtain a Pareto frontier solution set with more than 12 times the non-dominated solutions as a traditional ϵ-constraint method.
- *F2-Contribution 1:* This study introduces a novel simulation optimization framework for scheduling interruptible loads that considers load variation. The proposed framework presents great potential for IL planning in future smart grids with energy consumption controllers (ECCs), which enable utility companies and third-party aggregators to receive and control the energy consumption of each device automatically. Furthermore, this doctoral research is the first study to utilize simulation, optimization, and simulation design-ranking algorithms in an integrated framework to offer robust ILM scheduling for the smart grids in detail (at the device level).
- *F2-Contribution 2:* The proposed simulation optimization framework is formulated as an optimization problem to minimize the total cost imposed on the system by ILM while satisfying the desired load curve in all time periods. F2 is compared to relaxed deterministic optimization, random search, and simulated annealing (SA) algorithms

for performance evaluation and gives quite promising results in terms of feasibility and the cost of resultant scheduling.

- *F1 & F2-Contribution*: The combination of F1 and F2 provides a comprehensive tool for energy providers to implement ILM and load shifting strategies in smart grids. These two frameworks also have the ability to consider both deterministic and uncertain cases, based on user preference.

Chapter 2

Background and Literature Review

A smart grid is an autonomous electricity environment able to deliver electricity in a controlled, smart way from points of generation to consumers. These consumers are considered an integral part of a smart grid because they can alter their purchasing patterns and behaviors based on received information, incentives, and disincentives (two-way communication) [13]. Smart grids are capable of improving reliability performance, customers' responsiveness, and encouraging greater efficiency decisions by the customers and the utility provider [14]. Smart grids play a critical role in transforming the traditional power grid system into a user-oriented service that provides high-security, high-quality, and efficient energy grids. Despite the significant advantages of smart grids, maintaining their sustainability requires the total capacity of installed generation in the system to be larger than the maximum load demand; this ensures the security of supply in the face of uncertainty (e.g. generation breakdowns and interruptions to primary fuel sources) and variations in demand due to adverse weather [15]. In the literature of energy management, DSM is found to be an efficient way to increase power grid reliability. Demand side management refers to a modification of normal consumption patterns of electrical usage by end-use customers in response to changes in the price of energy or to customer pay incentives in order to reduce electricity price and usage in periods with a high wholesale market price or lack of energy supply [16-18].The complete integration of DSM and smart grids requires communication systems and sensors, automated metering, intelligent devices, and specialized processors. DSM has great potential for energy grid reliability, in particular because of the invention of ECCs, that enables the energy providers to monitor the energy consumption of each device. By promoting customer interaction and

responsiveness, DSM determines short-term impacts on electricity markets, leading to economic benefits for both the clients and the service provider. Furthermore, DSM reduces overall plant and capital cost investments and postpones the need for network upgrades by improving the reliability of the power system [19, 20]. In response to customer participation in DSM programs, electricity consumption can change in three possible ways: (1) reduction of energy consumption through load curtailment strategies, (2) a partial shift in energy consumption to a different time period, and (3) utilization of backup energy generators such as diesel generators to limit dependence on the main grid [17]. Load curtailment can be attained by dimming lighting levels, decreasing the temperature set points of air conditioners, etc. On the other hand, shifting power consumption can be achieved by commercial and residential customers by pre-cooling facilities and shifting loads from higher- to lower-cost time periods [21].

Different DSM programs, shown in Fig. 3, can be divided into two main categories: incentive-based programs (IBPs) and price-based programs (PBPs) [22, 23]. Classical IBPs can either be direct load control (DLC) programs or interruptible/curtailable load programs. Market-based IBPs include emergency demand response (DR) programs, demand bidding, the capacity market, and the ancillary services market. In a classical IBP, which forms the core of this doctoral research, participating customers receive participation payments, usually as a bill credit or discount rate, for their involvement. In DLC programs, utilities can remotely shut down participant equipment on short notice. Typical remotely controlled equipment includes air conditioners and water heaters. This kind of program is of interest mainly to residential customers and small commercial customers.

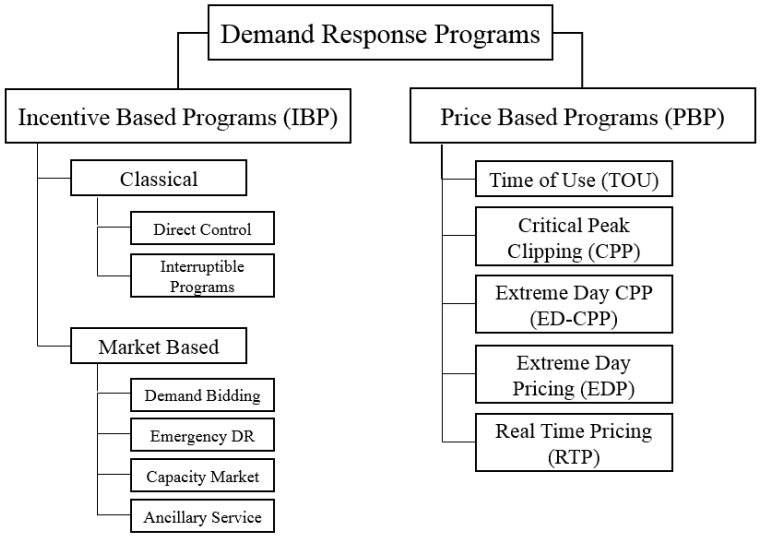

Fig. 3: Classification of demand response programs

C. W. Gellings has classified DSM (and primarily DLC) programs into six broad categories, as shown in Fig. 4 and explained below.

(1) Peak Clipping: Peak clipping is the reduction of peak load using DLC [1] and is mostly used in direct utility control of customers' appliances. In smart grids, load or appliance power can be altered via remotely controllable switches due to the high level of control. While DLC is known as a means to reduce peak capacity during peak periods and days, it also can be used to reduce operating costs and dependence on critical fuels [23].

(2) Valley Filling: In valley filling, low demand periods are filled by building off-peak capacities. This form of load management can be achieved using different types of energy storage such as water heating or space heating that can replace fossil fuel loads [22].

(3) Load Shifting: A standardized load shifting program shifts energy usage from peak periods to off-peak periods on a recurring basis, often by storing energy produced during off-peak hours and using this energy during peak hours to support loads [2].

(4) Strategic Conservation: This method aims to achieve load shape optimization by applying demand reduction methods directly on customer premises. The distribution management system considers this for longer-term implications of demand reduction on network planning and operation [24].

(5) Strategic Load Growth: This method optimizes daily response in case of significant demand beyond the valley filling technique. It is based on increasing the market share of loads supported by energy conversion and storage systems or distributed energy resources. A strategic load growth program is a planning method to balance increasing demand with processes for constructing necessary infrastructure that accompanies load growth. The future smart grid has to provide the necessary infrastructure for strategic load growth [9].

(6) Flexible Load Shape: Flexible load shaping is mainly related to the reliability of the smart grid. Smart grid management systems identify customers with flexible loads who are willing to be controlled during critical periods in exchange for various incentives.

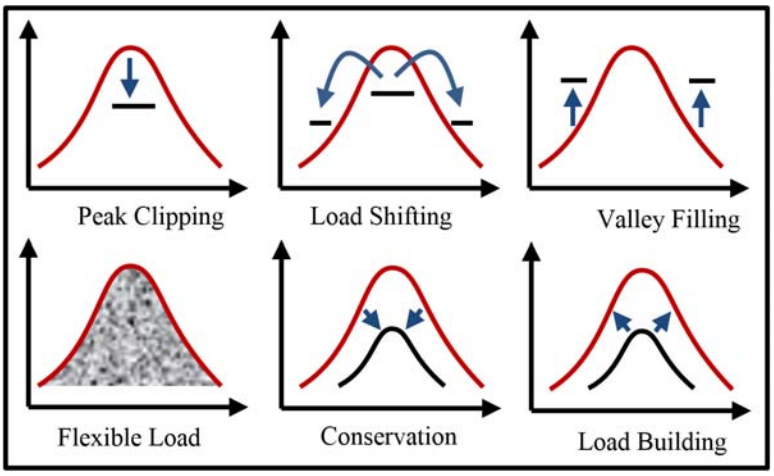

Fig. 4: The main DSM programs in energy management literature [1-9]

Of these DSM programs, peak clipping (also known as ILM) and load shifting have become a focus of attention due to their ease of application and high efficiency. Previous

studies about ILM and load shifting and their benefits and drawbacks are summarized in Tables 1 and 2.

Table 1: Selected ILM studies in the literature of energy management

Method	Main Idea	Benefits	Drawbacks
Single-objective optimization model for ILM using optimal power flow analysis [25]	Minimization of power generation cost and interruption cost for customers using optimization model	Ease of application and deterministic model	Not applicable to large problems and is a single-objective function
Optimization model for ILM in secondary reserve using ancillary service market [26]	24-hour-ahead ILM to minimize the cost	Considers dynamic price change as follows: $\beta_{i,T} = \beta_{0,T}\left(1 - \frac{R}{RLIM}\right)$	Requires high computation time due to multiple constraints; only considers minimization of cost
Model Reference Adaptive Control (MRAC) strategy using fuzzy dynamic programming [27]	Minimization of interruption cost using optimization model; fuzzy dynamic programming for interrupted loads	DLC optimization model to acquire optimal solutions; considers customer satisfaction using fuzzy set	Applies to small ILM problems and requires high computation time
Scheduling of interruptible loads using particle swarm optimization (PSO) [28]	Binary particle swarm optimization (BPSO) to schedule ILs (16h)	Metaheuristic algorithm acquires near-optimal solutions using ILM; applicable to large problems	Considers deterministic load demands and has only been tested on small problems
Minimization of cost for ILM and IL scheduling [29]	Optimization model with second-order polynomial model	Application of advanced ILM on industrial scale	Considers only industrial customers and only minimizes operational cost

Table 2: Selected load shifting studies in the literature of energy management

Method	Main Idea	Benefits	Drawbacks
Genetic algorithm (GA) for scheduling time-shiftable loads in smart grids [9]	Finding the near-optimal scheduling of time-shiftable loads on a device level	Considers smart grids with smart meters for mutual communication; tested on a smart grid case study	Only considers the minimization of cost as an objective function; GA does not guarantee the optimal solution
Incentive-based optimization model for DSM of PHEVs [30]	Optimization of PHEV fleet to minimize costs for energy supplier	Considers three-step framework for DSM including aggregation, optimization, and control; able to find scheduling for PHEVs	Proposed dynamic programming for PHEVs is not applicable to large-scale problems; limited to scheduling of PHEVs

Simulation model to use water heat pump and thermal energy storage (TES) for load shifting [31]	Heat-pump heating systems demonstrate ability to have active role in DSM programs	TES and water heat pump are more efficient ways to store energy than backup energy generators	Limited to thermal storage and satisfies energy storage planning
Load shifting in smart grids using glowworm PSO [32]	Utilizing load shifting strategy with the objective functions of annual energy loss minimization and fuel cost consumption minimization	One of the few studies that considers energy loss minimization as an objective function	Does not consider load shifting costs and only minimizes fuel cost
Simulation optimization model for load shifting in residential smart grid [33]	Utilizing micro-combined heat and power (CHP) for load shifting strategy in microgrid	Considers μ-CHP as a powerful tool for storing energy and implementing load shifting strategy	Uses single-objective function (cost) and deterministic values for device loads

In the literature of energy management, load shifting and ILM programs have been studied from several perspectives. Two critical assumptions have been considered in the literature of Energy load management: deterministic and uncertain energy load management. Despite the progress achieved in deterministic DSM literature, to the best of the author's knowledge, there is no study that considers both the energy provider's and customer's side. Furthermore, energy providers attempt to satisfy the desired load demand curve with minimal operational costs; however, less attention has been paid to customer satisfaction and emissions. Building on the contributions of the studies summarized in Tables 1 and 2, this doctoral research has two main sections: (1) a deterministic DSM framework that is responsible for load shifting and ILM programs considering deterministic loads for buildings and (2) a stochastic and dynamic simulation optimization ILM framework that investigates uncertainty in device loads. Investigation of robust DSM reveals that variations in different devices' energy consumption have not yet been considered. The assumption of constant energy consumption is critical for the DSM program's practicality and realism, but as in the real world, the hourly energy load

consumption of electrical devices can be altered by several factors (e.g., a device's selected program; different modes such as on, off, and standby; etc.). The second framework of this doctoral research (FII) incorporates the variation of device load as an additive variation factor and addresses it via extensive simulation experiments to generate loads, considering the normal load distribution for each device. The details of the proposed methodology are provided in the following chapter.

Chapter 3

A Dynamic Data-Driven Optimization Model for DSM in Operation Planning of Smart Grids

The efficient utilization of distributed generation resources (DGs) and DSM in large-scale power systems plays a crucial role in satisfying and controlling electricity demand in an economically viable and environmentally friendly way. However, uncertainties about electricity generation from DGs, variations in load demand, and conflicts in objectives (emissions, cost, etc.) pose significant challenges in determining the optimal operation planning of smart grids. In this chapter, a dynamic data-driven multi-objective optimization model for day-ahead operation planning for smart grids is provided to illustrate simulation and optimization for energy management and DSM implementation. The proposed approach in this chapter considers total cost and emissions as objective functions, with the integration of ILM as a DSM program, to find the best load scheduling for interruptible loads. A key goal of this chapter is to deliver a simulation and optimization approach as an essential basis for frameworks I and II.

The proposed simulation and optimization approach includes three modules that interact with each other: (1) a simulation module that captures the behaviors of operating components such as solar panels and wind turbines and provides the data for the optimization model; (2) an optimization module that determines the optimal operational plan, which includes the utilization of diesel generators, purchased electricity from a utility, and interrupted load, and considers the cost and emissions objective functions using the ϵ-constraint method; and (3) a rule-based, real-time decision-making module that adapts the operation plan from the optimization model based on dynamic data from the smart grid and sends the revised plan back to it. A schematic interaction of data and modules is illustrated

in Fig. 5. The proposed dynamic data-driven, multi-objective optimization model is explained briefly in the three following sections.

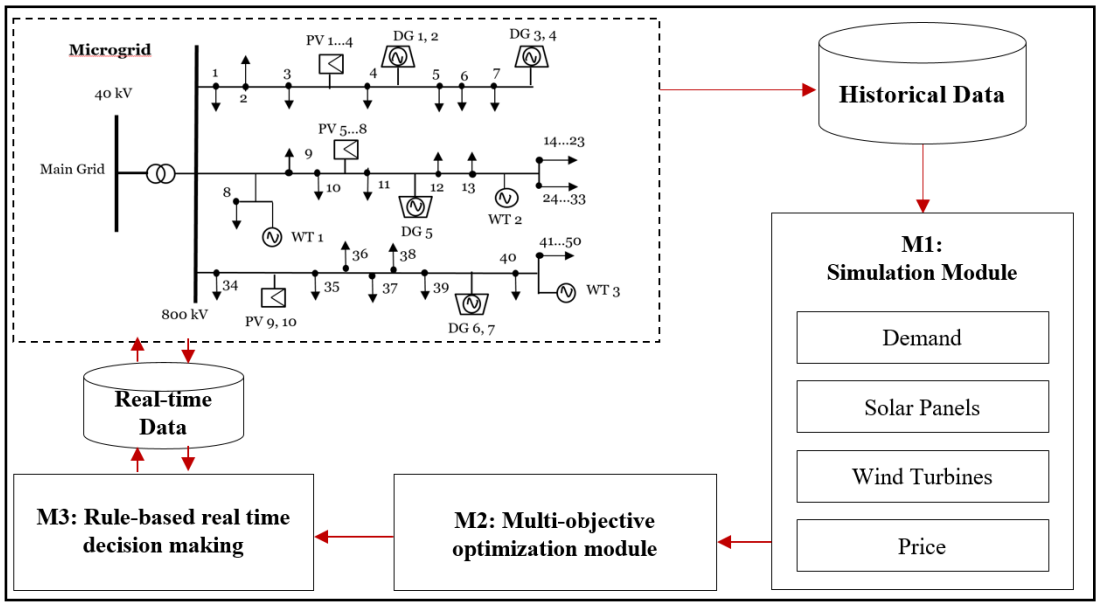

Fig. 5: Proposed dynamic data-driven multi-objective optimization for the smart grid

3.1. Simulation Module

The simulation module creates a valuable imitation of the operation of different components of smart grids while capturing uncertainty associated with these components, such as the intermittency of wind turbine energy generation. In this study, load demand, solar energy production, wind power generation, and hourly electricity prices are simulated as the smart grid operating components, as outlined below. Since other components, including diesel generators and the ILM program, are controllable components, they are taken into account only in the optimization model.

- Load demand: In this chapter, the demand data of smart gird buildings are assumed to follow the smart grid system in [34]. Notably, the forecasted hourly demand of each building (F_{it}) is a function of peak demand (PD_i) and the power factor (PF_{it}) of building i. Power factors are also determined based on customer type; values are

collected from [35] for residential customers and from [34] for commercial and industrial customers. Gaussian distribution is assumed in modeling demand uncertainty with 5% standard deviation as used in [36]. It is worthy to mention that the monthly power factors are utilized to differentiate the energy demand of each building monthly. The calculation of load demand for each hour and building is shown in (1).

$$F_{it} \sim N(\mu_{it}, \sigma_i) \; where \; \mu_i = \sum_{i=1}^{N} PD_i \times PF_{it} \; and \; \sigma_i = 0.05\mu_i \quad (1)$$

- Solar energy production: The power generation from solar panels depends on panel characteristics, solar irradiance, and ambient temperature as shown in (2-4). In these equations, the hourly solar generation (S_{out}) is a function of fill factor (FF), which is a constant related to panel characteristics, voltage (V), and current (I). Voltage and current are associated with attributes of the solar panel and cell temperature (T_c) calculated by the term $T_a + \frac{(T_n - 20)}{0.8} \cdot SI$ where T_a is ambient temperature, T_n is nominal cell temperature, and SI is solar irradiance.

$$S_{out} = FF \cdot V \cdot I \quad (2)$$

$$V = V_{oc} - k_v[T_c - 25] \quad (3)$$

$$I = SI \cdot (I_{sc} + k_i[T_c - 25]) \quad (4)$$

- Wind power generation: The power generation of wind turbines is calculated by a piecewise function that is dependent on the wind speed (v_w) at the site and the parameters of the power performance curve, which are rated power (P_w), cut-in speed (v_{ci}), cut-off speed (v_{co}), and rated speed (v_r). Total output power generated from the wind turbine (W_{out}) is computed as follows in (5) [37].

$$W_{out} = \begin{cases} 0 & if\ v_w < v_d \\ P_w \times \frac{v_w - v_{ci}}{v_r - v_{ci}} & if\ v_{ci} \le v_w \le v_r \\ P_w & if\ v_r \le v_w < v_{co} \\ 0 & if\ v_w \ge v_{co} \end{cases} \quad (5)$$

- Hourly electricity prices: The price of electricity from the main grid is modeled using historical data from [38]. In this study, it is assumed that hourly electricity prices for an entire month follow a similar pattern. In the calculation of prices, the data for the entire month are taken into account for each hour, and the best distribution is found using Bayesian Information Criteria [39, 40] among several distributions, including Weibull and Gamma. After this study's analysis, an Inverse Gaussian distribution is determined to be the best-fit distribution to explain hourly prices. The probability density function of the Inverse Gaussian distribution is given in (6).

$$f(x;\ \mu, \lambda) = \left[\frac{\lambda}{2\pi x^3}\right]^{1/2} exp\left(\frac{-\lambda(x-\mu)^2}{2\mu^2 x}\right) \quad (6)$$

3.2. Multi-Objective Optimization Module

After obtaining the load demand for each building, solar and wind power generation, and hourly electricity prices in the simulation module, the optimization module minimizes the cost and emission by determining the use of diesel generators, the amount of electricity purchased from the utility, and the schedule of interruptible loads under the ILM. As an incentive-based DSM program, ILM attempts to decrease the energy consumption of buildings during peak demand; however, energy providers must pay the interruption costs to consumers to encourage them to participate in this program. In this study, a bi-objective optimization model is formulated to minimize the cost and emission. It is important to point out that quadratic cost and emission functions of diesel generators are linearized using an

upper piecewise linear approximation method [41]; further explanation is provided in Chapter 4. While the cost function can be represented with one linear curve, the emission function can be converted into two linear curves called segments. The notations used in the model are shown in Table 3, and the model is represented by (7-20).

Table 3: Notations used in bi-objective optimization model

Indices	
i	Building number $i \in \{1, \dots, I\}$
t	Hours $t \in \{1, \dots, 24\}$
j	Diesel generators $j \in \{1, \dots, J\}$
k	Segments $k \in \{1, 2\}$
Parameters	
F_{it}	Forecasted load of building i at time t
D_t	Desired demand at time t (based on load demand, solar and wind generation)
PG_j^{min}	Minimum amount of electricity that can be generated by generation unit j
RI_{it}	Interruption rate ($/kW) (dependent on type of customer)
CS_j	Slope of cost function for generation unit j
CI_j	Intercept of cost function for generation unit j
ES_j^k	Slope of emission function for generation unit j at segment k
EI_j	Emission value for PG_j^{min}
GR_j^r	Reference for energy generation where $r \in \{1, \dots, k+1\}$
U_{lb}	Minimum amount that can be bought from utility
U_{ub}	Maximum amount that can be bought from utility
U_r	Energy rate (price) from utility
Variables	
g_{jt}^k	Energy produced by diesel generator g at time t and segment k
u_{jt}^k	Binary variable for the intercept of generation unit j at time t and segment k
x_{it}	Amount of interruption of building i at time t
b_t	Amount of electricity bought from utility
v_t	Binary variable for electricity from utility

Objective functions:

$$Min\ z_1 = \sum_{t=1}^{24}\Big[\sum_{i=1}^{I} x_{it}\ RI_{it} + \sum_{j=1}^{J}(u_{jt}\ CI_j + \sum_{k=1}^{2} g_{jt}^k\ CS_j) + U_{lb}\ U_r\ v_t + (b_t - U_{lb})U_r\Big] \quad (7)$$

$$Min\ z_2 = \sum_{t=1}^{24}\sum_{j=1}^{J}\sum_{k=1}^{2} g_{jt}^k\ ES_j^k + u_{jt}\ EI_j \quad (8)$$

Subject to:

$$D_t = \sum_{i=1}^{I} F_{it} - S_t - W_t \quad (9)$$

$$D_t - \sum_{i=1}^{I} x_{it} \leq \sum_{j=1}^{J}\left[\sum_{k=1}^{2} g_{jt}^{k} + u_{jt}^{1}\, PG_j^{min}\right] + b_t \qquad \forall t \quad (10)$$

$$g_{jt}^{k} \leq \left(GR_j^{k+1} - GR_j^{k}\right) u_{jt}^{k} \qquad \forall j, t \text{ and } k = 1 \quad (11)$$

$$u_{jt}^{k+1} \leq u_{jt}^{k} \qquad \text{where } k = 1 \quad (12)$$

$$\left(GR_j^{k+1} - GR_j^{k}\right) - gs_{jt}^{k} \leq M(1 - u_{jt}^{k+1}) \qquad \forall j, t \text{ and } k = 1 \quad (13)$$

$$x_{it} \leq 0.3 \cdot F_{it} \qquad \forall i, t \quad (14)$$

$$\sum_{t=1}^{24} x_{it} \leq 0.02 \sum_{t=1}^{24} F_{it} \qquad \forall i \quad (15)$$

$$b_t \geq U_{lb} \cdot v_t \quad (17)$$

$$b_t \leq U_{ub} \cdot v_t \quad (18)$$

$$u_{jt}^{k}, y_{it}, v_t \in \{0, 1\} \quad (19)$$

$$x_{it}, g_{jt}, g_{jt}^{k}, b_t \geq 0 \quad (20)$$

The first objective function (7) minimizes the total cost, including the interruption cost ($\sum_{t=1}^{24}\sum_{i=1}^{I} x_{it}\, RI_{it}$), linearized form of diesel generator cost ($\sum_{j=1}^{J}\sum_{t=1}^{24} u_{jt}\, CI_j + g_{jt}\, CS_j$), and electricity cost ($\sum_{t=1}^{24} U_{lb}\, U_r\, v_t + (b_t - U_{lb})\, U_r$) bought from the utility. Equation (8) minimizes the CO_2 emission of diesel generators. Equation (9) defines the desired demand at time t, which is the summation over time of forecasted loads minus generated energy from wind and solar at time t. Equation (10) prevents the model from exceeding the desired demand at time t. Since the linearized form of the emission function includes two segments, (11)–(13) ensure that the model does not assign any value to the second segment before fulfilling the first segment. Equations (14) and (15) ensure that the amount of interruption for each building satisfies hourly and daily regulations for ILM. A user can modify the parameters for the interruptible loads. Equations (17) and (18) show the upper

and lower limit, respectively, of the energy that can be bought from the utility. Finally, (19) and (20) are sign constraints. In this chapter, the ε-constraint method is used to obtain the Pareto frontier for the proposed mathematical model.

3.2.1. Multi-Objective Optimization via ϵ-Constraint Method

In this section, the ϵ-constraint method, first proposed by [42], is used to solve the bi-objective optimization model. In order to implement the ε-constraint method in the abovementioned optimization problem, the problem is first solved for each objective function separately to find the minimum and maximum value for each objective function (payoff table). Next, the secondary objective function is added to the optimization model as a constraint in order to formulate the optimization problem as a single-objective optimization (based on the primary objective). In this work, the cost and emissions objective functions are considered primary and secondary, respectively. Based on the payoff table, the range of the secondary objective function is divided into n equal intervals. Then, the new optimization problem that minimizes the cost is solved for n different right-hand side and left-hand side values of a constrained emission function in order to obtain n Pareto frontier solutions (Fig. 6).

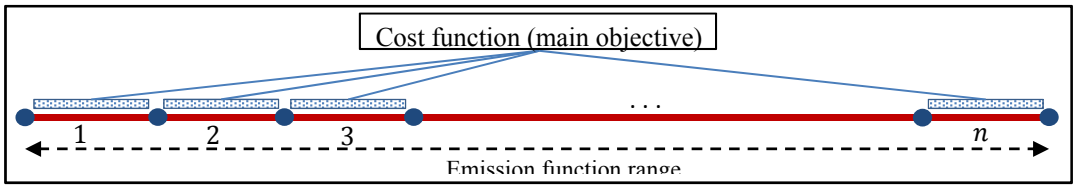

Fig. 6: Traditional ϵ-constraint method for bi-objective optimization

3.3. Real-Time Decision-Making Module

Load demand and generation from solar panels and wind turbines cannot be forecasted precisely, so the optimal solution based on simulation results requires modifications to adapt the solution to real-time data gathered from the smart grid. However, these modifications should satisfy the constraints without harming the optimal solution significantly. In this section, a rule-based real-time decision-making module (RTDM) is proposed to make precise decisions based on the real-time data from a smart grid, considering both cost and emission as it steps through time. The proposed rule-based RTDM is responsible for decisions regarding utilization of diesel generators, ILM and the amount of electricity bought from the main grid (Fig. 7). It should be noted that the algorithm is terminated if $\Delta D_t = 0$ at any checkpoints.

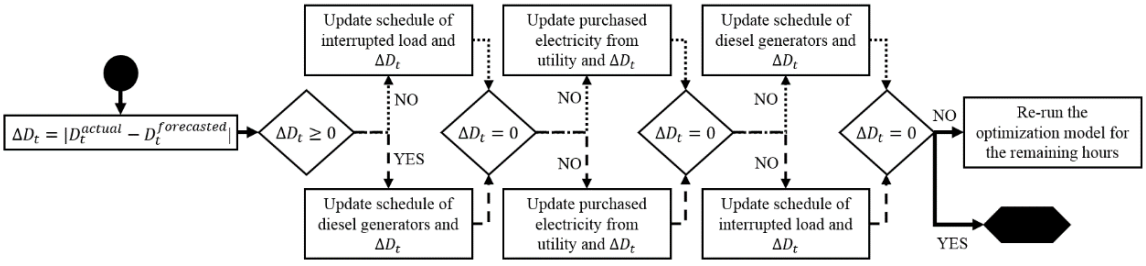

Fig. 7: Rule-based real-time decision-making module for smart grid operational planning

3.4. Experiments and Results

In order to present the capabilities and performance of the proposed approach, a case study of a synthetic smart grid was carried out. The smart grid analyzed in this chapter included 50 buildings composed of 35 residential, 10 commercial, and 5 industrial types of load profiles; solar panels that have a total capacity of 10 MW; three wind turbines; and seven diesel generators from four different types of thermal generators. The characteristics of the solar panels and wind turbines used in this study are shown in Table 4. Moreover,

the values for diesel generators were obtained based on the results of a piecewise linear approximation method; they are shown in Table 5.

Table 4: Attributes of wind turbines and solar panels [43]

Solar Panel		**Wind Turbine**	
Attribute	**Value**	**Attribute**	**Value**
Open circuit voltage	21.98 V	Turbine capacity	3000 kW
Short circuit current	5.32 A	Cut-in speed	4 (m/s)
Voltage temperature coefficient	14.4 mV/^{o}C	Cut-out speed	25 (m/s)
Current temperature coefficient	1.22 mA/ ^{o}C	Rated speed	16 (m/s)
Nominal cell operating temperature	43 ^{o}C	-	-
Fill factor	0.17	-	-

Table 5: Attributes of diesel generators

Thermal Generators				
Attribute	**Gen. Type I**	**Gen. Type II**	**Gen. Type III**	**Gen. Type IV**
Number of generators	2	2	1	2
Minimum power generation (MW)	50	40	30	20
Maximum power generation (MW)	300	250	175	120
Fixed cost ($)	16.52	12.02	9.89	7.47
Variable cost coefficient	0.0224	0.0229	0.0235	0.0223
Emission value for minimum power generation	0.88	0.76	1.01	0.66
Emission coefficient for segment I	0.0277	0.0214	0.0277	0.0195
Emission coefficient for segment II	0.0599	0.0432	0.0459	0.0364

As mentioned earlier, due to weather changes and variations in customer load profiles, the operation plans are different on any day of the year. However, it is commonly believed that changes within a season have minimal impact. Therefore, this study presents results of the proposed approach for the two best representative days of each season, which are July 15 in the summer and January 15 in the winter. First, the simulation model determined the hourly forecasted demand for each building and hourly solar and wind generation

according to the data shown in Tables 4 and 5. It should be noted that weather data were obtained from the Florida Automated Weather Network (FAWN) subsidiary of the University of Florida [44], and winter and summer electricity prices were determined using an Inverse Gaussian distribution where parameters are estimated based on historical data. Then the simulation results were sent to the bi-objective optimization model, which was solved for each objective function to construct the payoff table shown in Table 6.

Table 6: Resulting payoff table for bi-objective optimization model

Summer	Cost	Emission	Winter	Cost	Emission
Cost	$1,320.59	6.71 kg	Cost	$1,077.07	5.39 kg
Emission	$2,597.00	4.78 kg	Emission	$2,218.76	3.51 kg

In this study, the cost function has been selected as the primary objective function. The emission function is embedded in the model as a constraint as shown in (21).

$$\sum_{t=1}^{24}\sum_{j=1}^{J}\sum_{k=1}^{2} g_{jt}^{k}\, ES_{j}^{k} + u_{jt}\, EI_{j} \geq LB_{emission} \qquad (21)$$

In order to use the ϵ-constraint method, the emission function range ([4.78, 6.71] for summer and [3.51, 5.39] for winter) was divided into 100 intervals, and the optimization problem for minimizing the cost was solved for every interval by using A Mathematical Programming Language (AMPL) software on a computer with an i7 processor and 16 GB RAM. Based on the results of the optimization problem, the Pareto frontier was obtained in less than a minute and is represented in Fig. 8. Then, the best compromise solution was selected by determining the knee solutions, which are the preferred trade-off solutions in the Pareto frontier [45]. Since the primary objective here is to minimize cost, the knee solutions with a better total cost were chosen as the best compromise solutions for winter and summer.

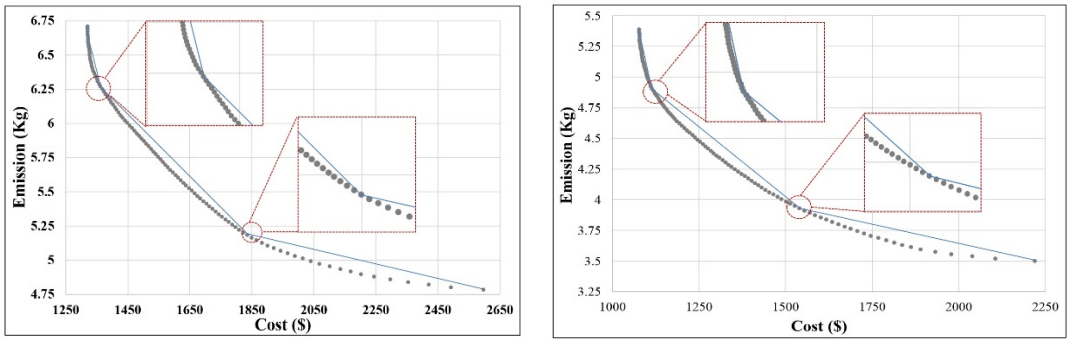

(a) Summer (b) Winter

Fig. 8: Resulting Pareto frontier from multi-objective optimization model

Based on the selected solutions, the optimal operation plans for summer and winter are shown in Fig. 9. It should be noticed that in both cases, there is unused generator capacity, showing that the smart grid has enough resources for electricity generation. In fact, even during peak hours in the summer, use of generator type I, which has the highest capacity, does not exceed a total of 60%. From Fig. 9 it can be understood that in the winter, the smart grid does not need electricity from the main grid, while in the summer, the smart grid buys electricity from the main grid for four hours a day. However, during these hours, the smart grid can produce its own energy. This study also demonstrates that the total amount of interrupted electricity is tiny for both seasons, meaning that the smart grid can satisfy customers regarding their electricity production. Finally, although generation from renewable energy sources in summer is almost twice the generation from renewable energy sources in winter, the higher demand in the summer leads to a higher cost and more emissions than in the winter.

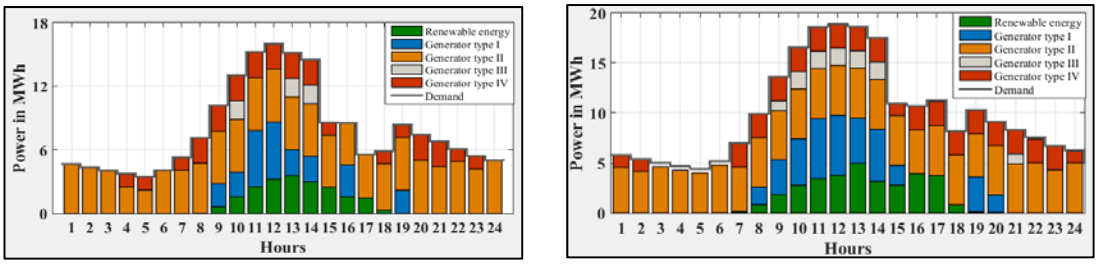

(a) Winter (b) Summer

Fig. 9: Resulting operation planning of the best compromise solutions

In the next step, dynamic data-driven multi-objective module (DDD-MOM) collects real-time data from the smart grid, and the RTDM adapts the best compromise solution from the optimization module based on these data. In this study, real-time smart grid data were simulated using slightly different parameters from those used in the simulation module. The results of the RTDM can be seen in Fig. 10, which shows that the changes in the cost function value between the optimization module solution and the RTDM solution reach, at most, a level of 0.9% in the summer and 0.6% in the winter. The differences in the emission values obtained from the optimization model and actual case are less than 0.4% in the winter and 0.6% in the summer. Hence, it can be concluded that the results obtained from the optimization model are robust regarding cost and emission objectives against uncertainties of power generation from renewable energy resources and load demand in real-time operation.

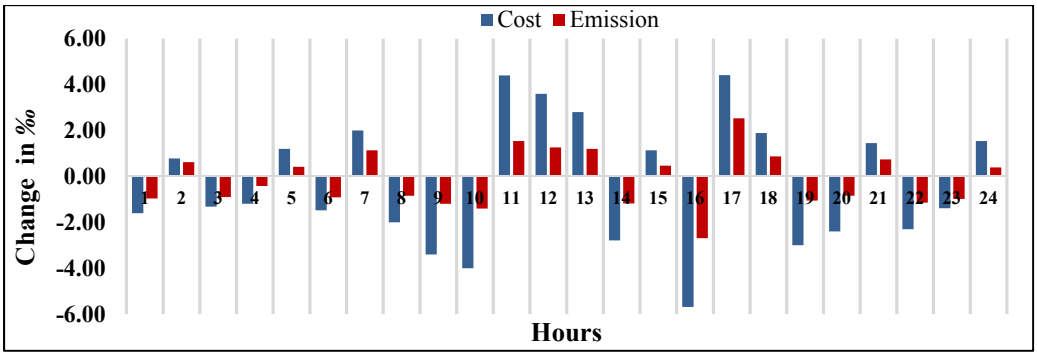

(a) Winter

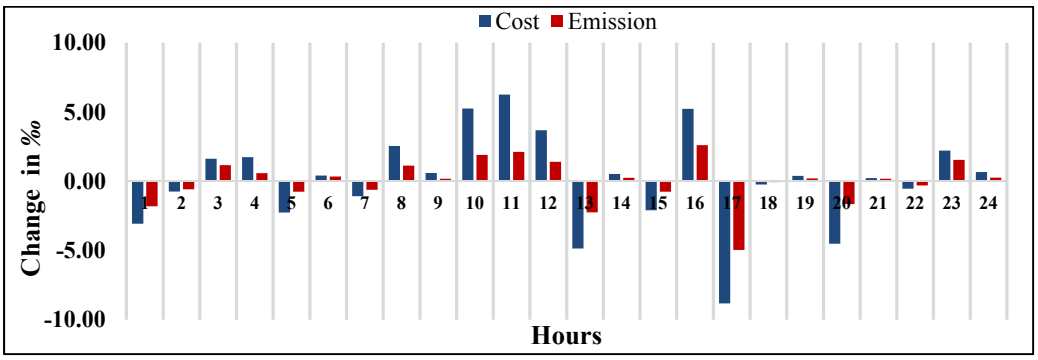

(b) Summer

Fig. 10: Results of RTDM model

Chapter 4

Deterministic Multi-Objective Optimization Problem for DSM (*F1*)

Demand side management is a superior tool for maintaining the sustainability and security of power systems during capacity shortage and emergency situations. It includes intentional modifications to electricity consumption patterns of end-use customers to alter the level of demand and timing of consumption. In addition to maintaining system sustainability, energy providers primarily need to minimize total cost and maximize customer satisfaction to encourage participation in DSM programs. This chapter proposes a multi-objective optimization model for load shifting and ILM with three objective functions. The first objective function minimizes the total cost of energy systems including costs of load shifting (or interruption) and thermal generators; the second objective function maximizes customer satisfaction (utility); and the third objective function minimizes the GHG emission of thermal generators. The components of the proposed framework are described in detail in the sections below.

4.1. 24-hour-ahead Energy Load Forecasting

Electricity load forecasting is one of the most important requirements for energy management and operation planning in the electrical sector. While several load forecasting methods have been developed in the literature of energy management, none can be generalized as the most efficient tool for all demand patterns [46-51]. In order to obtain a forecasted day-ahead load profile for buildings, we collected a large set of residential, commercial, and industrial electrical devices based on historical data. The forecasted hourly demand of each building (F_{it}) is a function of the peak demand (PD_i) and power factor (PF_{it}) of building i, and building load demand was obtained using the information

provided in Chapter 3. The calculation of load demand for each hour and building is shown in (22).

$$F_{it} \sim N(\mu_{it}, \sigma_i) \quad where \quad \mu_i = \sum_{i=1}^{N} PD_i \cdot PF_{it} \quad and \quad \sigma_i = 0.05 \cdot \mu_i \tag{22}$$

Furthermore, historical data about device electricity usage was used to capture actual customer energy consumption. The resulting datasets were used to obtain the day-ahead load forecasting generated by the simulation of historical data. The prediction method based on historical device data enables a user to identify devices with a possibility for load shifting and create a day-ahead load profile.

4.2. Mathematical Formulation of the Extended Operation Planning Problem

This chapter proposes a multi-objective optimization framework for operation planning problems that use the load shifting program in smart grids. The framework has three objectives: (1) minimization of total cost of energy systems, including costs of the load shifting program and thermal generators; (2) maximization of customer satisfaction (utility); and (3) minimization of GHG emissions from thermal generators. Notations used in the proposed model are shown in Table 7.

Table 7: Summary of notations and formulations used in the proposed deterministic DSM

Indices	
i	Buildings $i \in \{1, \dots, I\}$
j	Generation units $j \in \{1, \dots, J\}$
k	Segments $k \in \{1, 2, 3\}$
t	Hours $t \in \{1, \dots, 24\}$
w	Diesel generators ($w = 1, \dots, W$)
c	Customer types $c \in$ {industrial, commercial, residential}
Parameters	
a_w, b_w, c_w	Variable cost parameters of thermal generator w
CS_j	Slope of cost function for generation unit j
CI_j	Intercept of cost function for generation unit j
D_t	Desired demand at time t

ES_j^k	Slope of emission function for generation unit j at segment k
EI_j	Emission value for PG_j^{min}
F_{it}	Forecasted load for building i at time t
GR_j^r	Reference for energy generation where $r \in \{1, \dots, k+1\}$
L	Maximum allowed time for shifting
PG_j^{min}	Minimum produced energy for generation unit j
RS_t	Shifting rate (\$/kW)
RG_t	Diesel generator rate at time t (\$/kW)
S_w	Fixed cost of thermal generator w
UI_i	Intercept of utility function for building i
UR_i^r	Reference for utility function where $r \in \{1, \dots, k+1\}$
US_i^k	Slope of utility function for building i at segment k
$\alpha_w, \beta_w, \gamma_w, \psi_w, \lambda_w$	Emission parameters of thermal generator w
Variables	
g_{jt}	Produced energy by diesel generator g at time t
g_{jt}^k	Produced energy by diesel generator g at time t and segment k
$P_{G_{kt}}$	Energy generated in diesel generator k at time t
s_i^k	Shifted percentage of building i at segment k
$s_{it_1t_2}$	Shifted amount of load in building i from time t_1 to time t_2
S_c	Total percentage of shifted load in customer type c
u_{jt}	Binary variable for the intercept of generation unit j at time t
u_{jt}^k	Binary variable for the intercept of generation unit j at time t and segment k
v_i^k	Binary variable for the intercept of utility function building i at segment k

The first objective function for load shifting is composed of two different sources of costs: (1) cost to the system from using a load shifting DSM program and (2) the energy costs of diesel generators (fuel costs and startup costs). Hence, the first objective function can be written as (23).

$$Min\ Z_1 = \sum_{t_1=1}^{24} \sum_{t_2 \in \{t_1-L,\dots,t_1+L\}} s_{it_1t_2} \cdot RS_i + \sum_{t=1}^{24} \sum_{w=1}^{W} (a_w + b_w P_{G_{wt}} + c_w P_{G_{wt}}^2 + S_w) \quad (23)$$

To obtain the load shifting cost, we consider both forward and backward load shifting using summation over i, t, and k for $s_{it(t-k)}$ and $s_{it(t+k)}$. The second part of (1) measures

the amount of cost for energy generation in thermal generators, which is composed of fuel cost ($a_w + b_w P_{G_{wt}} + c_k P_{G_{wt}}^2$) and setup cost ($S_w$).

The second objective function minimizes the environmental GHG emission caused by thermal generators. The total tonnage of emissions per hour can be calculated as (24). Parameters α_w, β_w, γ_w, ψ_w, and λ_w are emission coefficients that are different for each type of diesel generator. It should be noted that emission function can be converted to a cost function by using the emission tax rate; however, cost imposed to the system is not the only aspect of GHG emission in this study.

$$Min\ Z_2 = \sum_{t=1}^{24} \sum_{w=1}^{W} 10^{-2}\left(\alpha_w + \beta_w P_{G_{wt}} + \gamma_w P_{G_{wt}}^2\right) + \psi_w e^{\lambda_w P_{G_{wt}}} \quad (24)$$

The third objective function represents customer satisfaction via utility function. [52] has shown that the marginal benefit for energy customers follows (25), in which θ and s are customer parameters.

$$B(\theta, q) = \theta b_0 q - \frac{1}{2} s \theta q^2 \quad (25)$$

Fig. 11(a) illustrates the marginal benefit for risk seeker and risk averse customer types ($b_0, s = 1, \theta = 0.5,1$). As can be seen, more energy consumption for customers results in more satisfaction.

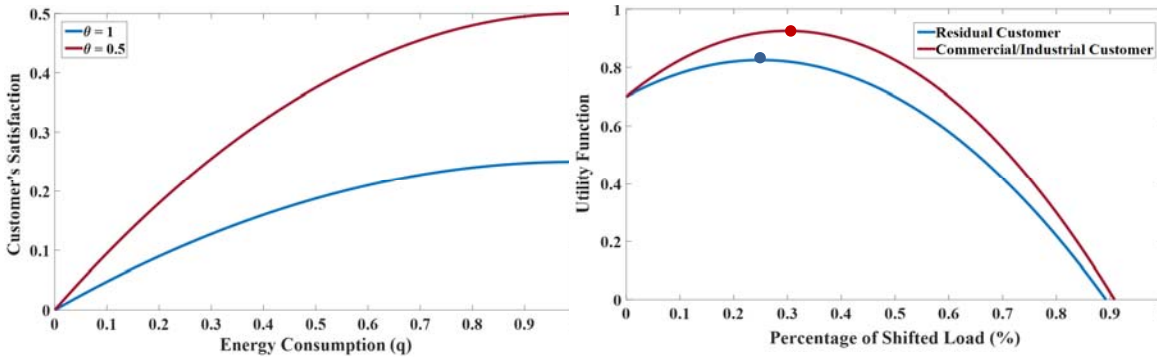

(a) **(b)**

Fig. 11: (a) Customer benefit vs energy consumption, (b) Utility function

Since power plants provide incentives for load shifting programs, customers are more willing to participate. Incentives increase customer satisfaction (utility function) up to a specific percentage of the shifted load (red and blue points in Fig. 11[b]); however, if the amount of shifted load exceeds that point, customer satisfaction (utility function) starts decreasing. After preliminary experiments, (26) is obtained as the customer utility function, and the utility function is shown in Fig. 11(b). In equation (26), S_c represents the total percentage of shifted load in customer type c that can be acquired via summation over shifted loads ($s_{it_1t_2}$) during a 24-hour time period for each customer type ($\sum_{i\in c}\sum_{t_1=1}^{24}\sum_{t_2\in\{t_1-L,\dots,t_1+L\}} s_{it_1t_2}$).

$$\text{Max } Z_3 = a \cdot S_c^2 + (-1-a)\cdot S_c + U_0 \tag{26}$$

In order to satisfy the desired demand in all time periods, (27) ensures that the energy load at time t is lower than desired load demand and backup energy generation. In order to find the total load at time t, the shifted load from time t ($\sum_j s_{ijt}$) is subtracted from the forecasted load, and then the shifted load is added to time t ($\sum_k s_{itk}$). The load at time t must be lower than the available energy that includes desired demand and backup energy

generation (energy produced by diesel generators = $D_t + \sum_{w=1}^{W} P_{G_{Wt}}$). This constraint is written as (27).

$$\sum_{i=1}^{n}\left[F_{it} - \sum_k s_{itk} + \sum_j s_{ijt}\right] \leq D_t + \sum_{w=1}^{W} P_{G_{Wt}} \quad \forall t \tag{27}$$

In this problem, we assume that loads cannot be shifted forward or backward more than L time periods (where L indicates the maximum number of hours a customer is willing to shift his or her energy consumption). The constraint can be written as (28).

$$|j - k| \leq L \tag{28}$$

The power output of each diesel generator must not exceed its lower boundary or its higher boundary. The related constraint can be written as (29).

$$P_w^{min} \leq P_{G_w} \leq P_w^{max} \tag{29}$$

Lastly, (30) ensures a positive value for the variables of the model.

$$s_{ijk}, g_t \geq 0 \tag{30}$$

4.3. Piecewise Linear Approximation Method

Linear programming is the most suitable modeling tool to solve complex problems, and it provides a fast and efficient way to obtain results. However, as stated previously, the second and third objective functions of the proposed deterministic framework are in nonlinear forms. Nonlinear functions are often encountered in power system optimization. In this doctoral study, an effective piecewise linear (PWL) approximation technique is used to linearize the nonlinear objective functions. Piecewise linear approximation for the linearization of nonlinear equations is widely used in several fields of science [39-41]. PWL functions allow arbitrary functions to be represented to any accuracy by increasing the number of segments until the desired accuracy is met. The extensive use of PWL approximation is due to this method's advantage in linearizing nonlinear equations in

different regions efficiently (with a low computational burden) and its ability to decide on the size of the subspaces [53]. This study linearizes convex and concave nonlinear functions differently. A function f: $\mathbb{R}^n \xrightarrow{\Delta} \mathbb{R}$ is called convex if $\forall x, y \in \mathbb{R}^n$, and $\forall \lambda \in [0,1]$,

$$f(\lambda x + (1-\lambda)y) \leq \lambda f(x) + (1-\lambda) f(y)$$

The PWL approximation of convex objective functions and constraints is shown in Fig. 12(a). It is important to point out that the linear estimation of the emission function is always a conservative overestimation to consider the worst possible scenario for minimization. As seen in Fig. 12(a), GHG emission is converted to three linear sub-functions for three different ranges of energy generation (ranging from P_{min} to P_{max}).

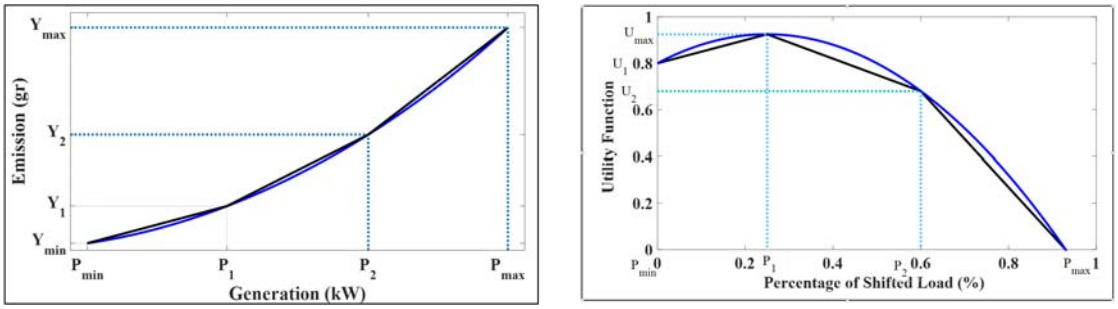

Emission Function (Convex) Utility Function (Concave)

Fig. 12: Linear forms of the (a) emission function and (b) utility function

The PWL approximation for concave nonlinear objective functions is shown in Fig. 12(b). The linear approximations of utility functions are underestimated (below the nonlinear utility function curve) to ensure the maximization of utility. As can be seen in

Fig. 12, the utility function is divided into three linear functions, which means that the utility function can be rewritten as three linear functions for three shifted load ranges.

4.3.1. Linearized Form of the Extended Operation Planning Problem

After the implementation of the PWL approximation on the proposed deterministic multi-objective optimization for the load shifting problem, the linearized form of the optimization model can be written as (31-43). The notations used in the linearized model are provided in Table 7, and the MILP formulation of the multi-objective DSM problem is as follows:

Objective Functions:

$$Min\ z_1 = \sum_{t_1=1}^{24}\sum_{i=1}^{I}\sum_{t_2\in\{t_1-L,\dots,t_1+L\}} s_{it_1t_2}\cdot RS_i + \sum_{j=1}^{J}\sum_{t=1}^{24} u_{jt}\,CI_j + g_{jt}\cdot CS_j \quad (31)$$

$$Min\ z_2 = \sum_{t=1}^{24}\sum_{j=1}^{J}\sum_{k=1}^{3}(g_{jt}^{k}\cdot ES_j^k + u_{jt}\cdot EI_j) \quad (32)$$

$$Min\ z_3 = \sum_{i=1}^{I}\sum_{k=1}^{3}(s_i^k\cdot US_i^k + UI_i) \quad (33)$$

Subject to:

$$\sum_{i=1}^{I}\Big[F_{it} - \sum_{t_1\in\{t-L,\dots,t+L\}} s_{itt_1} + \sum_{t_2\in\{t-L,\dots,t+L\}} s_{it_2t}\Big] \le D_t + \sum_{j=1}^{J} g_{jt},\ \ \forall\, t \quad (34)$$

$$\sum_{k=1}^{3} g_{jt}^{k} + u_{jt}\cdot PG_j^{min} = g_{jt}, \forall\, j \text{ and } t \quad (35)$$

$$g_{jt}^{k} \le \left(GR_j^{k+1} - GR_j^{k}\right)\cdot u_{jt}^{k} \quad (36)$$

$$u_{jt}^{k+1} \le u_{jt}^{k} \quad \text{where } k \in \{1,2\} \quad (37)$$

$$\sum_{k=1}^{3} u_{jt}^{k} \le 3u_{jt} \quad (38)$$

$$\sum_{t=1}^{24}\sum_{t_2\in\{t-L,\dots,t+L\}} s_{itt_2} = \sum_{t=1}^{24} F_{it}\cdot\sum_{k=1}^{3} s_i^k \quad (39)$$

$$s_i^k \le \left(UR_i^{k+1} - UR_i^{k}\right)\cdot v_i^k \quad (40)$$

$$v_i^{k+1} \leq v_i^k \quad \text{where } k \in \{1,2\} \tag{41}$$

$$u_{jt}, u_{jt}^k, v_i^k \in \{0,1\} \tag{42}$$

$$s_{it_1,t_2}, s_i^k, g_{jt}, g_{jt}^k \geq 0 \tag{43}$$

Equation (31) is the linearized form of (23), which is composed of two parts. The total cost of the shifting program ($\sum_{t_1=1}^{24}\sum_{i=1}^{l}\sum_{t_2\in\{t_1-L,\dots,t_1+L\}} s_{it_1t_2}.RS_i$) remains as in (23) since it is in a linear form; the second part is the linearized form of the cost function of energy generation from diesel generators obtained by PWL approximation ($\sum_{j=1}^{J}\sum_{t=1}^{24} u_{jt}\, CI_j + g_{jt}\, CS_j$). In order to linearize the diesel generator costs, two variables (u_{jt} as a binary variable and g_{jt} as generated energy) and two parameters (CI_j for the intercept and $CS_j$for the slope of the linear form of energy generation cost) are defined. Similar to (31), (32) is the linearized form of the emission objective function obtained by using two parameters for slope and intercept of each segment (ES_j^k and EI_j, respectively) and two variables (g_{jt}^k and u_{jt}). The utility function is linearized in three segments as shown in (33) using the slope and intercept of each linearized segment. It should be noted that the utility (satisfaction) of customers is calculated using the percentage of shifted energy (s_i^k). Equation (34) ensures that the energy load is lower than the desired demand and backup energy for all hours ($t = 1, \dots, 24$) and each load cannot be shifted more than L time periods. Equation (35) attempts to obtain energy generation for thermal generator j (g_{jt}), and it also ensures that energy generation is above the minimum amount (PG_j^{min}). Equation (36) guarantees that diesel generator j generates equal to or less than the maximum capacity. Equation (37) ensures that diesel generator j does not proceed to the next linear segment before fulfilling the current segment. Similarly, (38) ensures that diesel

generator j does not exceed the maximum energy generation capacity. Equation (39) defines the percentage of the shifted load for each hour in each building (s_i^k). Similar to (36), (40) prevents the utility function from reaching a value higher than the upper limit in each segment. Equation (41) prevents the next segment of the utility function from getting a value before fulfilling the current utility function. Equations (42) and (43) are constraints for non-negativity and the integrality of variables.

4. 4. An Advanced Augmented ϵ-constraint for Multi-Objective Optimization

This doctoral dissertation proposes a novel multi-objective optimization method, which is an advanced version of the augmented ϵ-constraint method first developed by [42]. In the context of multi-objective optimization, ϵ-constraint and weighting methods are among the most useful methods. The ϵ-constraint method has several advantages over the weighting method: (1) The weighting method considers the original feasible region and results in extreme solutions (linear problems), while the ϵ-constraint method alters the feasible region and is able to generate non-extreme efficient solutions; (2) in the weighting method, the assigned weights of objective functions have a strong effect on the obtained result, while in the ϵ-constraint method, there is only need to identify the objective function with the highest priority; and (3) in the ϵ-constraint method, the number of generated solutions can be controlled by adjusting the number of grid points. This section first provides a brief explanation of the conventional ϵ-constraint method and then discusses the details of the improved ϵ-constraint method. Let (44) denote the multi-objective mathematical programming problem.

$$\max \left(f_1(x), f_2(x), \dots, f_{\mathcal{P}}(x)\right) \quad \text{st:} \tag{44}$$

$x \in \mathcal{S}$

In the optimization problem, x represents the vector of decision variables, $\mathcal{S}$ shows the solution space, and $f_p(x)$ represents the p^{th} objective. It is assumed that the p^{th} objective has the highest priority among all objectives. In the augmented ϵ-constraint method, the multi-objective optimization problem is transformed into a single-objective problem by setting up the p^{th} objective, which has the highest priority as an objective function, converting other objectives to constraints, and adding these constraints to the original constraint set. The new optimization problem is shown in (45).

$$\begin{aligned} &\max f_p(x) \\ &\text{st:} \\ &f_k(x) \geq \epsilon_k \quad k \in \{1, \dots, p-1, p+1, \dots, n\} \\ &x \in \mathcal{S} \end{aligned} \tag{45}$$

In Equation (45), ϵ_i represents the right-hand-side value for the constraint associated with the i^{th} objective. It should be noted that the value of each new constraint shows the value of its corresponding objective function. After the new optimization problem is obtained using the augmented ϵ-constraint method, the ϵ values for each constraint are updated to obtain the Pareto frontier. Here, as a first step, the range of $f_i(x), \forall i \in \{1, \dots, \mathcal{P}\}\backslash\{p\}$ (the minimum and maximum value of each objective function) is calculated by optimizing the problem with each objective function (constructing a payoff table). To this end, (45) is optimized for each objective function separately, and the values of each objective function are stored in a payoff table (see Table 8).

Table 8: Payoff table for objective functions

	$f_1(x)$	$f_2(x)$	…	$f_{p-1}(x)$	$f_{p+1}(x)$	…	$f_k(x)$
$\max f_1(x)$ st: $x \in \mathcal{S}$	f_1^*	f_2^1	…	f_{p-1}^1	f_{p+1}^1	…	f_k^1
$\max f_2(x)$ st: $x \in \mathcal{S}$	f_1^2	f_2^*	…	f_{p-1}^2	f_{p+1}^2	…	f_k^2
$\max f_3(x)$ st: $x \in \mathcal{S}$	f_1^3	f_2^1	…	f_{p-1}^3	f_{p+1}^3	…	f_k^3
…	…	…	…	…	…	…	…
$\max f_k(x)$ st: $x \in \mathcal{S}$	$f_1^{\mathcal{P}}$	$f_2^{\mathcal{P}}$	…	f_{p-1}^k	f_{p+1}^k	…	f_k^*

In Table 8, each row shows the values of each objective corresponding to the given optimization problem. In addition, f_i^j denotes the value of the i^{th} objective when the j^{th} objective is optimized with respect to original constraint set.

After obtaining the range of each objective function in the payoff table, the augmented ϵ-constraint method uses a greedy approach to obtain the Pareto frontier, where the range of the i^{th} objective function is divided into q_i equal intervals by using $(q_i - 1)$ intermediate equidistant grid points. As a result, $\prod_{i\in\{1\dots p\}\setminus\{k\}} q_i$ optimization problems have to be solved to find the Pareto optimal set, which requires high computational time to find the Pareto frontier set. In addition, this greedy approach can result in dominated solutions in $\prod_{i\in\{\{1\dots p\}\setminus\{k\}\}} q_i$ runs. Additionally, the performance of the ϵ-constraint method depends on the selection of equidistant intervals. Larger intervals might result in a smaller number of Pareto frontier solutions, while smaller intervals increase the number of non-dominated solutions and the computational burden. In order to address these issues, this study proposes an advanced ϵ-constraint method, which updates the ϵ values of constraints that correspond to objectives by using sensitivity analysis. After obtaining the payoff table and the main objective function (the objective function with the highest priority), this proposed method differs from the augmented ϵ-constraint method proposed by [42] for updating the ϵ values of constraints associated with objectives. In this thesis, the idea is that instead of

using predefined ϵ values, the ϵ values of binding constraints are updated using sensitivity analysis to obtain the exact points that result in different solutions for the Pareto solution set. In linear programming, changing the right-hand side of a constraint by Δ does not affect the basic solution. For instance, this study wants to obtain the Pareto frontier solution set for a multi-objective optimization problem with three objective functions. In this case, the range of objective functions in the payoff table is used as constraints. Using the ϵ-constraint model, the range of each constraint is divided into $q_{in} - 1$ intervals, using q_{in} equidistant points. However, obtaining a high number of dominated solutions is the main problem of the ϵ-constraint method. In order to overcome this problem using this thesis's proposed method, gridding for each constraint can be implemented by using Δ values obtained from the sensitivity analysis (see Fig. 13). This gridding ensures that by changing the right-hand side (RHS) of each constraint in the range of $[\epsilon_1, \epsilon_1 + \Delta)$, the optimal solution does not change. However, changing the RHS to $\epsilon_1 + \Delta + \delta$ $(0 < \delta)$ results in different non-dominated Pareto solutions, where δ is a sufficiently small number to avoid obtaining the same solution. Accordingly, by changing the RHS of other constraints (transformed from objective functions) using Δ values and solving the main problem (31) iteratively, the Pareto solutions can be obtained. Sensitivity analysis can easily be implemented via optimization software such as AMPL or General Algebraic Modeling System (GAMS)without requiring high computational resources.

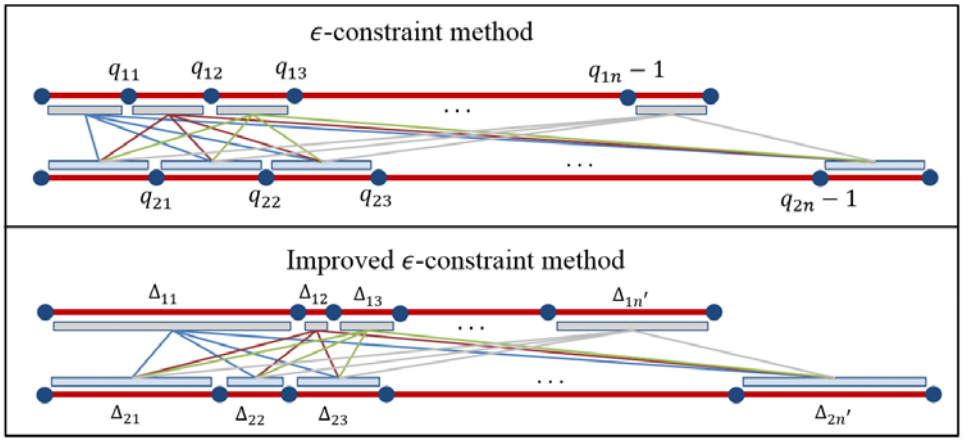

Fig. 13: ϵ-constraint method vs. proposed improved ϵ-constraint method

Fig. 14 illustrates the proposed optimization method in a flowchart. The proposed algorithm starts with constructing a payoff table by separately solving the optimization problem for each objective. Based on the obtained payoff table, the range for each objective function can be acquired. In the next step, considering the $k-1$ objective functions as constraints, Δ for each constraint is obtained by conducting a sensitivity analysis in any optimization software. As can be seen in Fig. 14, Δ_{i+1}s is calculated for each constraint until the value of the acquired Δ becomes greater than the upper bound (e_i). The algorithmic steps of the proposed methodology are shown in Fig. 15.

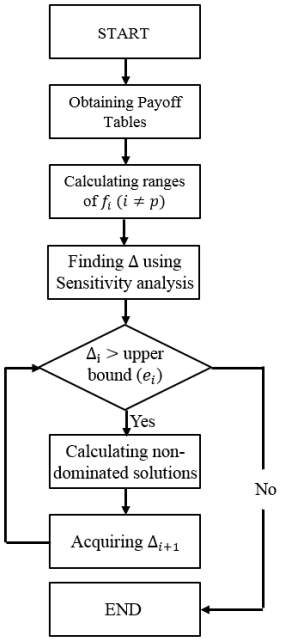

Fig. 14: Flowchart of the proposed improved $\boldsymbol{\epsilon}$-constraint method

[Step 1]: Input data

(1) Defining parameters of the problem F_{it} (forecasted load in department i at time t), D_t (desired demand at time t), RS_t, RG_t, RI_t(shifting, backup, and interruption rates), and L (maximum allowed shifting time)

(2) Reading D_t and F_{it} from excel (text) file

[Step 2]: Acquiring payoff table

(1) Calculation of optimal solution of the problem with each objective function separately and acquiring f_1^*, f_2^*, and f_3^*.

(2) Finding the range of objective functions.

[Step 3]: Finding the Pareto frontier solutions
While $RHS_2 \geq LHS_2$ repeat [1-5]

(1) Optimizing the problem with f_2 and f_3 as constraints

While $RHS_3 \geq LHS_3$ repeat step [2-3]

(2) Finding Δ_2 and Δ_3 using sensitivity analysis
(3) Set $LHS_3 \leftarrow LHS_3 - \Delta_3$
(4) Set $LHS_2 \leftarrow LHS_2 - \Delta_2$

Fig. 15: Advanced $\boldsymbol{\epsilon}$-constraint algorithm for multi(3)-objective optimization

4.5. Experiments and Results

In order to demonstrate the performance and capabilities of the proposed framework, a case study of a synthetic smart grid with 50 buildings, including 35 residential, 10 commercial, and 5 industrial buildings, was used. Forecasted loads and desired demands based on historical data for the considered smart grid are shown in Fig. 10. Fig. 16 shows that, on a typical day, forecasted loads are higher than desired demand between 10:00 A.M. and 8:00 P.M. Thus, the extra loads must be covered either by the load shifting program to alter final energy consumption close to the objective load curve or by the energy generation from diesel generators to satisfy the extra loads.

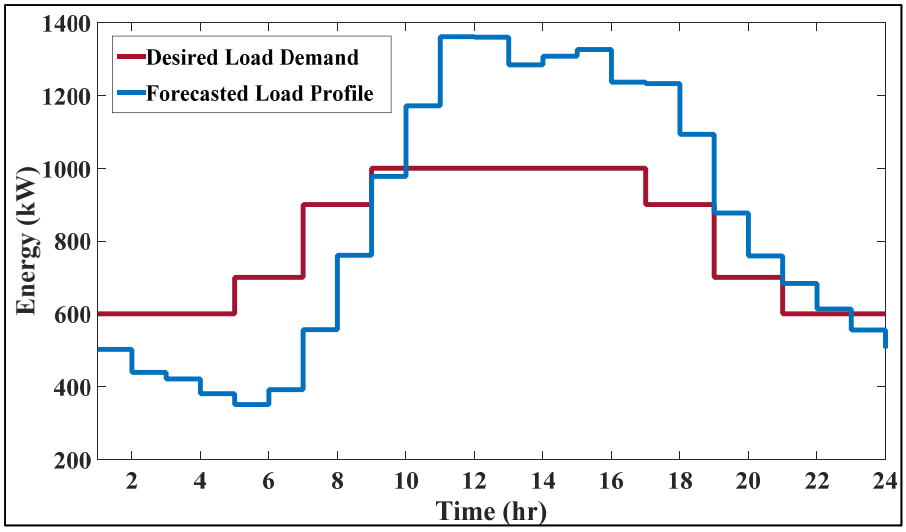

Fig. 16: Load demand vs. desired demand for 24 hours

In this study, four types of diesel generators (two of type I, two type II, one type III, and two type IV) were considered, and the characteristics of the utilized diesel generators are provided in Table 9. It should be noted that the emission coefficient for the linearized form of the emission function (ES_j^k) is provided in the last three rows of Table 9.

Table 9: Attributes of diesel generators

Thermal Generators				
Attribute	**Gen. Type I**	**Gen. Type II**	**Gen. Type III**	**Gen. Type IV**
Number of generators	2	2	1	2
Minimum power generation	50	40	30	20
Maximum power generation	300	250	175	120
Fixed cost	16.52	12.02	9.89	7.47
Variable cost coefficient	0.0224	0.0229	0.0235	0.0223
Emission value for minimum power generation	0.88	0.76	1.01	0.66
Emission coefficient for segment I (ES_j^1)	0.164	0.0283	0.0184	0.022
Emission coefficient for segment II (ES_j^2)	0.0273	0.0465	0.0314	0.0417
Emission coefficient for segment III (ES_j^3)	0.0398	0.0465	0.0477	0.647

The proposed model attempts to satisfy the forecasted load when considering three objectives: cost minimization, GHG emission minimization, and customer utility maximization. As explained in Section 4.4, an advanced ϵ-constraint method is used to solve the multi-objective optimization. As a first step, the multi-objective model was solved for each objective function to create a payoff table. The payoff table for the optimization model is provided in Table 10.

Table 10: payoff table for the proposed problem

	$f_1(x)$	$f_2(x)$	$f_3(x)$	Solution time (s)
Min Cost	548.59	5718.71	-0.17	0.99
Min Emission	939.64	214.96	-2.46	0.81
Max Utility	4446.92	35342.16	0.10	0.16

As discussed in Section 4.4, each column shows the value of the objective function value for each objective with respect to the single-objective problem shown in Table 6. It should be noted that the values for utility function (fourth column) were obtained without fixed values (U_0 in equation [26]), which is why negative values occurred without affecting the optimal solution. Then, the obtained results were used in the proposed advanced ϵ-constraint to obtain the Pareto frontier solutions. The proposed method was implemented using AMPL software, and the results are illustrated in Fig. 17. In order to compare the quality of solutions, Pareto frontier solutions obtained from the proposed advanced ϵ-constraint are compared to those from classical ϵ-constraint method results in Fig. 17.

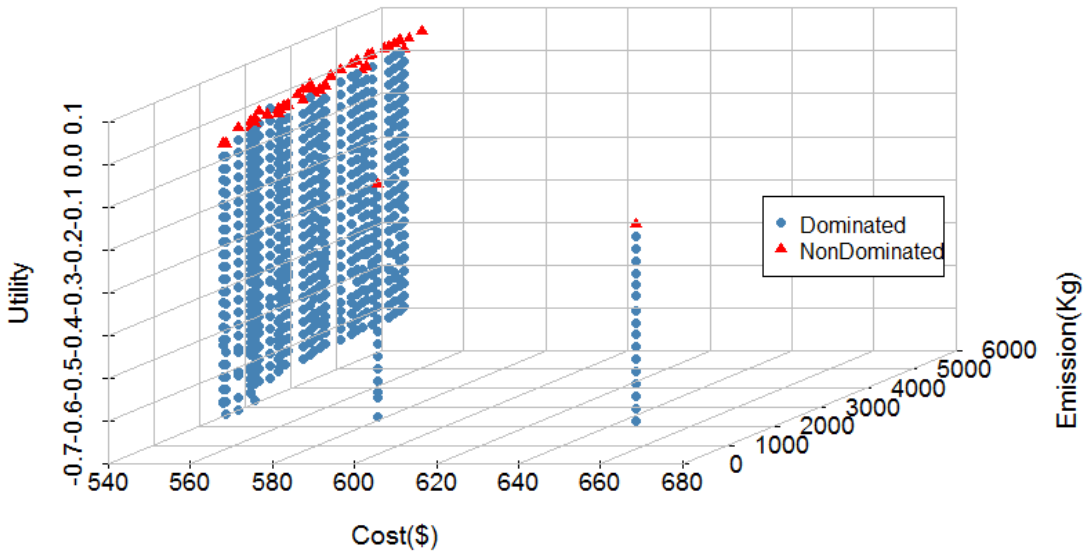

(a)

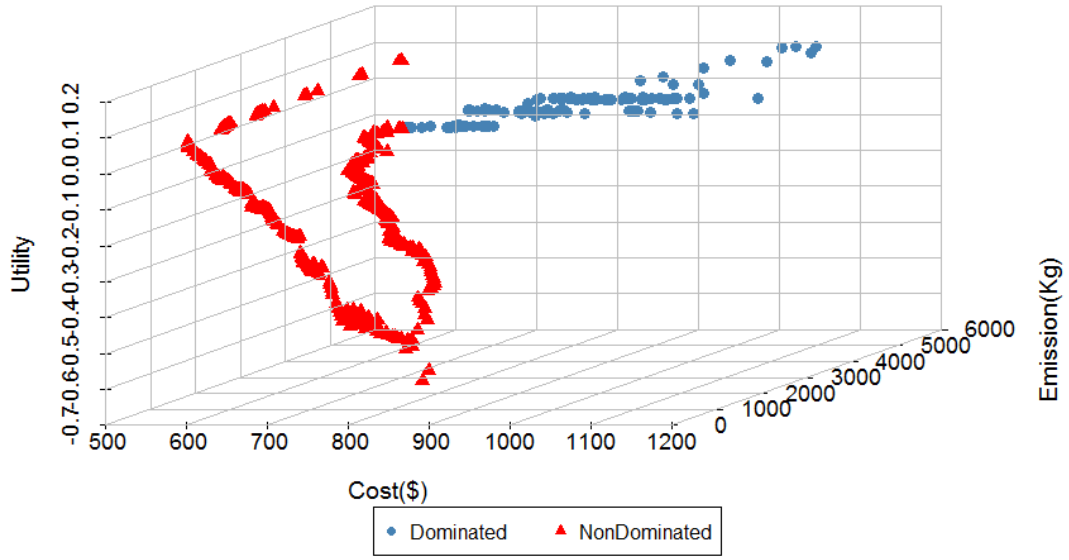

(b)

Fig. 17: Pareto frontier solutions for the (a) classical $\boldsymbol{\epsilon}$-constraint method and (b) advanced $\boldsymbol{\epsilon}$-constraint method

As can be seen in Fig. 17, the proposed advanced ϵ-constraint method resulted in a significantly higher number of non-dominated solutions, while most of the solutions obtained using the classical ϵ-constraint method were dominated solutions. In order to obtain the Pareto frontier solutions using the classical ϵ-constraint method, considering

cost as the main objective function, the obtained ranges of emission and utility functions (from the payoff table) were divided into 25 and 30 equidistant intervals, respectively. Thus, in total, there were 750 (25*30) optimization problems to solve. Since gridding is based on equidistant intervals, the solution for each interval can result in dominated solutions (see the vertical consecutive red points in Fig. 17(b)). On the other hand, the proposed ϵ-constraint method determines intervals based on a sensitivity analysis, which results in new non-dominated solutions. As a result, the advanced ϵ-constraint method resulted in 78.62% non-dominated solutions, while the classical ϵ-constraint method resulted in 5.6% non-dominated solutions. Here, further analysis indicated that the alternate optima in the solution space can cause the dominated solutions in the Pareto frontier obtained from our proposed method. In addition to a higher number of non-dominated solutions resulting from the proposed method, the average and total computational times were lower than in the classical ϵ-constraint (Table 11 and Fig. 18). The solutions obtained from these two methods are provided in Appendix II.

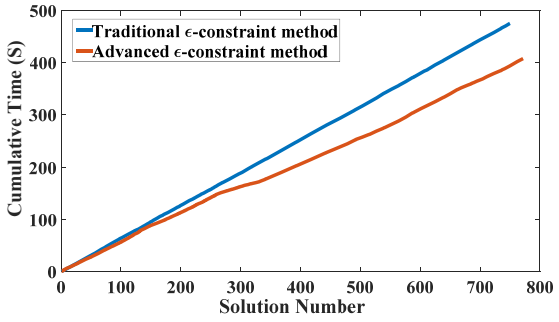

Fig. 18: Comparison of computational time

Table 11: Time comparison of solutions

	ϵ-constraint	Proposed method
Total Time (seconds)	473.87	407.641
Average Time	0.6146	0.5280
Number of Non-dominated Solutions	42 out of 750	607 out of 772
% of Non-dominated Solutions	5.6%	78.62%

Fig. 19 illustrates the resulting load curve obtained from the proposed operation planning framework using the advanced ϵ-constraint method. The blue line represents the results of the best compromising solution obtained from the proposed method (out of 607 non-dominated solutions). The comparison of the load profile before and after

implementing the proposed load shifting framework reveals that the proposed program managed to decrease thermal energy generation in the time periods of 10:00 A.M.–3:00 P.M. and 9:00–10:00 P.M. by shifting loads to earlier or later time periods. It is important to point out that limitations on the load shifting range ($L = 3$) did not allow the model to shift loads to the time period of 12:00–5:00 A.M., and this is the reason to have spare capacity during these hours. Since satisfying the required curtailment improves grid sustainability and reduces the need to construct under-utilized energy facilities with enormous costs, and the amount of thermal energy generation is decreased significantly, the proposed multi-objective operation planning framework successfully reduces the peak load demand of the smart grid.

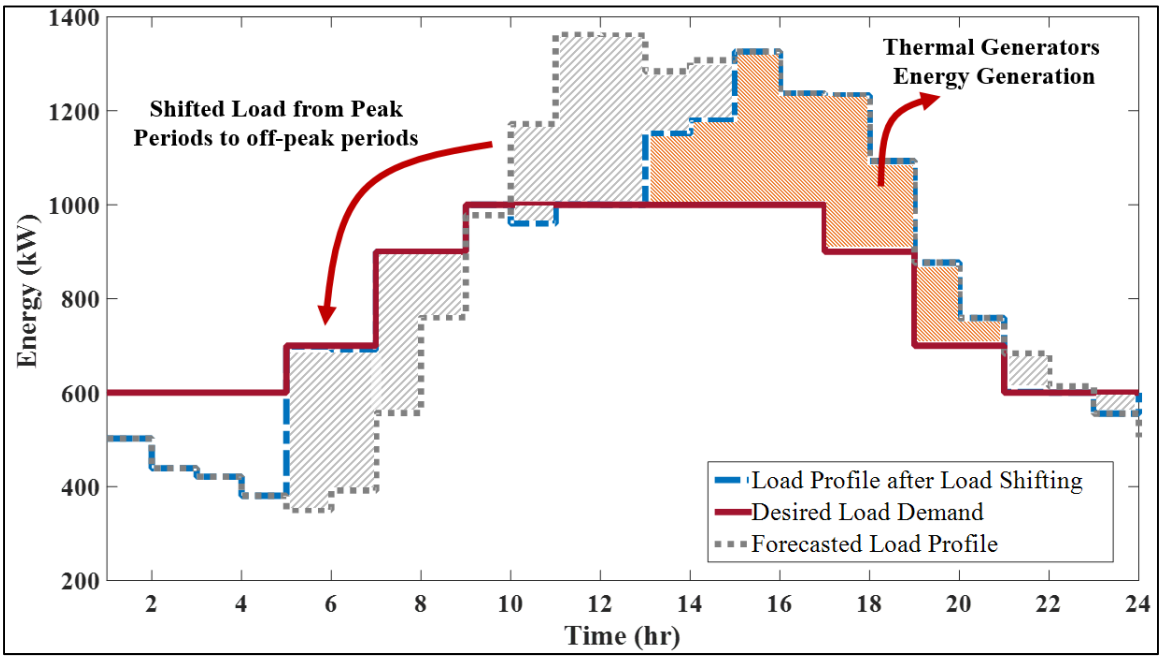

Fig. 19: Comparison of forecasted load profile, desired demand, and load profile after implementing the proposed framework

Chapter 5

Simulation and Optimization Framework for ILM in Smart Grids with Uncertain Loads (F2)

This chapter of the doctoral dissertation proposes a novel evolutionary simulation and optimization framework for ILM in smart grids with uncertain loads in order to find (near-)optimal schedules for ILs, given device loads with uncertainty. Scheduling ILs with load uncertainty is a complex, single-objective stochastic optimization problem. Here, the goal is to minimize the total cost of interruption as in (46), while satisfying the hourly required load curtailment as in (47). Equation (48) satisfies the limitation of the number of interruptions, and (49) ensures that the number of ILs is equal to or less than the number of working devices. The considered problem is formulated as an integer program involving uncertain parameters ($C_k^{\pm}$), where the required curtailment for each hour is formulated as a soft constraint. The notations and mathematical formulations for the scheduling of the interruptible loads problem (SILP) are shown in Table 12 and (46-50), respectively.

Table 12: Summary of notations for SILP [14]

Indexes	Description
$\boldsymbol{k}$	Device type where $k \in K$, and $K \in \{1, \dots, N\}$
$\boldsymbol{t}$	Hour where $t \in T$, and $T \in \{1,2, \dots ,24\}$
Parameters	Description
$\boldsymbol{R_k}$	Interruption cost of device type k ($/device)
$\boldsymbol{C_k}$	device load of type k
$\boldsymbol{D_t}$	Desired demand at time t
$\boldsymbol{n_k}$	Number of devices of type k
$\boldsymbol{\mathrm{off}_k}$	Maximum off-time for device type k
$\boldsymbol{f_{kt}}$	Number of working devices of type k at time t according to forecasting values
Binary variables	Description
$\boldsymbol{x_{kt}}$	Number of interrupted devices of type k at time t where $k \in K$ and $t \in T$

Objective function:

$$Min \ \sum_{k=1}^{N} \sum_{t=1}^{T} x_{kt} \ . R_k \ . \ C_k^{\pm} \tag{46}$$

St.:

$$\sum_{k=1}^{N} (f_{kt} - x_{kt}) \cdot C_k^{\pm} \leq D_t \qquad \text{for } \forall t \in T \tag{47}$$

$$\sum_{t=1}^{T} x_{kt} \ \leq \ \text{off}_k \, . n_k \tag{48}$$

$$x_{kt} \leq \ f_{kt} \qquad \text{for all } k \text{ and } t \tag{49}$$

$$x_{kt} \ \in \ \mathbb{Z}^+ \qquad \text{for all } k \text{ and } t \tag{50}$$

The objective function of SILP (24) minimizes the total cost of the interruption of devices, where the superscript " $\pm$ " denotes the considered additive variation for each device. Equation (47) ensures that the necessary load curtailment is satisfied at each time period t (hour). Equation (48) prevents the model from frequently interrupting a specific device due to low interruption costs (i.e., having a low interruption price during all shortage periods). Equation (49) prevents the model from interrupting non-working devices, and (50) ensures integer values for the variables of this problem. This chapter first provides an overview of the proposed framework, and Section 5.2 explains the proposed simulation optimization framework and its components in detail.

5.1. Overview of the Simulation-Optimization Framework

The proposed evolutionary simulation and optimization framework for ILM is composed of three main elements: 1) a genetic algorithm that progressively discovers new solutions for the scheduling of ILs, 2) a simulation model that determines the performance of different interruption scenarios, and 3) a complete ranking OCBA that optimizes the allocation of the number of replications dedicated to each simulation scenario and identifies the top m-best solutions for the genetic algorithm. The framework is initiated by a set of

initial n random solutions obtained by the genetic algorithm. These solutions represent a schedule of devices that need to be interrupted in pre-specified time periods. Then, the simulation model evaluates these solutions for a predetermined initial number of replications to acquire a mean and variance for the performance of each individual solution. Here, a solution's performance is different in every replication due to energy consumption variation. Using the computed mean and variance performances of each solution, the OCBA algorithm returns the optimal number of additional simulation replications that need to be allocated to each solution. This procedure is repeated until the total budget (i.e., the number of the maximum allowed replications) is reached. Then, the complete ranking of these solutions is acquired by the OCBA and is provided to the genetic algorithm. In each iteration, the genetic algorithm keeps the best m solutions and produces a new set of solutions using its crossover and mutation operators until the population is fulfilled. In the next step, the simulation and OCBA cooperate to determine a complete ranking of these solutions using the minimum number of replications. This procedure continues until a predetermined number of iterations is reached. In the following section, the proposed framework and its components are described in detail.

5.2. Components of the Simulation Optimization Framework

The elements of the proposed simulation and optimization framework are described in detail as the following:

- *Genetic Algorithm for SILP*: Inspired by the Darwinian evolutionary theory, the genetic algorithm is a population-based metaheuristic algorithm widely used in various combinatorial problems [54]. The proposed evolutionary simulation and optimization framework for ILM is initialized by generating a set of feasible solutions with the

genetic algorithm for the predefined SILP (GA_{SILP}). Here, an individual composed of genes denotes a particular solution for a given problem, and the performance function is used to evaluate the efficiency of solutions (i.e., a value of fitness). The GA_{SILP} starts with an initial population that evolves into better solutions through its subsequent generations. The evolution process in this study's genetic algorithm has four steps: 1) a selection step that chooses solutions with superior performance value; 2) a diversification step, which ensures that the generated solutions are disparate in order to avoid local optimal solutions; 3) a crossover operator that recombines more than two individuals to form a new population; and 4) a mutation operator that alters the individuals to maintain diversity in the population. Due to the uncertainty of the load among different devices, a range is needed to define the performance function of each solution, and a constant load value is not adequate.

Since SILP is a constrained optimization problem with uncertain parameters, the proposed GA_{SILP} improves the feasibility of solutions. Here, (49) is satisfied with crossover and mutation operators. However, these operators may not satisfy (47) and (48). Controlling the feasibility of the required curtailment constraint is another challenging task when using analytical operators due to the load uncertainties. In order to address these two issues simultaneously, a performance (fitness) function is built to consider not only the objective function of the problem but also penalty costs for infeasible constraints as shown below.

$$P_f = \sum_{k=1}^{N}\sum_{t=1}^{24} x_{kt}\cdot R_k + p_r \cdot \left(\sum_{t=1}^{24} \max\left(Req_t - \sum_{k=1}^{N}(f_{kt} - x_{kt})\cdot C_k^{\pm}, 0\right)^2\right) + p_m \cdot \left(\max\left(\sum_{t=1}^{24} x_{kt} - off_k\right), 0\right) \quad (51)$$

Equation (51) calculates the performance function (P_f) of each interruption schedule. The first term of the equation, $\sum_{k=1}^{N}\sum_{t=1}^{24} x_{kt} \cdot R_k$, is the objective function of the problem. The second term, $p_r \cdot (\sum_{t=1}^{24} \max(Req_t - \sum_{k=1}^{N}(f_{kt} - x_{kt}) \cdot C_k^{\pm}, 0)^2)$, gradually penalizes infeasible schedules when they do not satisfy the required load curtailment constraint. The more the load deviates from the desired curve, the more the infeasible solution is penalized. The last term, $p_m \cdot (\max(\sum_{t=1}^{24} x_{kt} - off_k),0)$, calculates the penalty for solutions that violate the maximum number of off-times. p_r and p_m are the user-defined penalty parameters with large values used to discard infeasible solutions for the next replication of GA$_{SILP}$.

In order to evaluate the fitness functions of the GA$_{SILP}$'s solutions in each iteration, a complete ranking OCBA is used to rank all solutions and assign simulation replications for each design in an efficient manner, as described in the next subsection. Once a full ranking of the solutions is obtained, the top m best-ranked solutions are kept for the next iteration of the genetic algorithm. Furthermore, additional m random solutions are added to diversify the new solution set (and avoid local optima). As a result, $2m$ solutions, including the top m ranked solutions from the previous step and m random solutions from the current step, are kept. Next, in order to fill the solution set, $\binom{2m}{2}$ solutions are generated by applying crossover and mutation operators over the stored $2m$ solutions.

In the GA$_{SILP}$, solutions are stored in matrices with 24 columns (representing a 24-hour period) and N rows (representing the N different types of devices). While traditionally, a binary string is used to represent the solutions, higher cardinality representations can also be used [55], where each entry in a representation matrix can take values

in $\{0, 1, \dots, f_{kt}\}$. This representation offers the capability of developing problem-specific crossover and mutation operators. Here, a crossover operator is defined as one that takes a convex combination of parent matrices ($\vec{a}$ and $\vec{b}$) and rounds it to the nearest integer to generate the new solutions ($c = \|\lambda a + (1-\lambda)b\|$, where $\vec{c}$ is the new solution and λ is a random number between 0 and 1, as shown in Fig. 20).

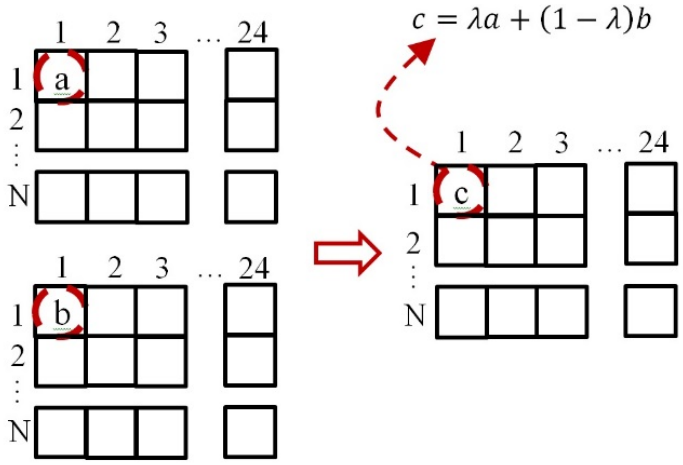

Fig. 20: Proposed crossover function

- *Simulation and Design Ranking Algorithm for ILM*: Recent advances in simulation and computing power area make it possible to solve complex stochastic systems previously thought impossible. The proposed simulation and optimization framework in this doctoral research was built using Java-based software (Anylogic 7) that is responsible for evaluating the different interruption scenarios. Every type of device is modeled as a simulation agent that requires a specific amount of power to operate. These agents can be turned on and off depending on the interruptive scheduling that is fed into the simulation from the GA component. Additionally, there is an agent for the utility company that supplies power to the device agents. At the end of the specified time period (24 hours), the utility agent calculates the performance function of the given

interruptive schedule. However, there is uncertainty on the device loads, and as a result, every scenario (solution fed from the genetic algorithm to the simulation) needs to be simulated several times to obtain a performance with a high confidence level. A screenshot of the Anylogic model designed for this simulation and optimization model is shown in Fig. 21.

Fig. 21: Screenshot of proposed simulation and optimization framework in Anylogic

To accelerate the computational time of the simulation optimization process and improve the efficiency of the simulation, several simulation design-ranking and selection procedures have been applied in past studies [56-62]. [58, 59] introduce the ranking and selection methods by using multiple statistical comparisons among the simulation designs. These methods can only be applied to small-scale problems with finite designs, but they planted the seeds for further research. Later, [57] proposes the OCBA method, which obtains results from a simulation model that evaluates the performance of alternative designs and allocates further replications for each design based on the mean and variance of the performance values [56]. OCBA has been the focus for several researchers and has been applied to several different problems. Recently, [62] has extended the OCBA method by proposing an efficient simulation OCBA procedure to rank all simulation designs (alternatives). Following the footsteps of [62], this dissertation incorporates the OCBA for complete ranking into a genetic algorithm to increase the efficiency of the selection process.

In this proposed simulation and optimization framework, genetic solutions' fitness functions are ranked. Fig. 22 illustrates the procedure of a complete ranking OCBA algorithm, considering $\alpha = (\alpha_1, \dots, \alpha_k)$ as a proportion of the total budget to be allocated to each design (chromosome) with $\sum_{i=1}^{k} \alpha_i = 1$ and $\overline{X_{f_i}}(\alpha_i n) = \sum_{j=1}^{\alpha_i n} X_{f_{ij}} / \alpha_i n$ as the sample mean fitness value for solution i where n represents the total number of solutions at each iteration (generation population).

[Step 1]: Input data

(3) Define k (number of alternative designs), T (total simulation budget), Δ (available budget for one iteration of the algorithm), n_0 (initial replications for each design), and l (current iteration in OCBA)

(4) Set $l \leftarrow 0$;

(5) Set $n_1^l = n_2^l = \cdots = n_k^l = n_0$

While $\left(\sum_{i=1}^{k} n_i^l < T\right)$ repeat Steps [2]-[3]

[Step 2]: Additional budget calculation

(3) Increase computing budget by Δ using new budget using asymptotically optimal allocation (AOA):

$\sum_i \alpha_i = 1,$

for any $i \neq j$ the allocation from AOA is such that:

$$\min\left(\frac{(\mu_{f_{i-1}} - \mu_{f_i})^2}{\sigma^2_{f_{i-1}}/\alpha^*_{i-1} + \sigma^2_{f_i}/\alpha^*_i}, \frac{(\mu_{f_i} - \mu_{f_{i+1}})^2}{\sigma^2_{f_i}/\alpha^*_i + \sigma^2_{f_{i+1}}/\alpha^*_{i+1}}\right) = \min\left(\frac{(\mu_{f_{j-1}} - \mu_{f_j})^2}{\sigma^2_{f_{j-1}}/\alpha^*_{j-1} + \sigma^2_{f_j}/\alpha^*_j}, \frac{(\mu_{f_j} - \mu_{f_{j+1}})^2}{\sigma^2_{f_j}/\alpha^*_j + \sigma^2_{f_{j+1}}/\alpha^*_{j+1}}\right)$$

(4) Additional budget for each design can be obtained by using $\alpha^* = (\alpha_1^*, \alpha_2^*, \ldots, \alpha_k^*)$:

$$n_i^{l+1} = \alpha_i^* . (\sum_{i=1}^{k} n_i^l + \Delta)$$

[Step 3]: Simulation

(5) Perform additional $\left[\max\left(n_i^{l+1} - n_i^l, 0\right)\right]$ simulation replications for all design k

(6) Set $l \leftarrow l + 1$.

Fig. 22: Complete ranking OCBA algorithm

5.3. Experiments and Results

In order to demonstrate the effectiveness of the proposed framework, a case study of a synthetic smart grid was conducted using a real set of data. The set of data for devices, including their types, capacities, the maximum number of interruptions, interruption rates, and the possibility of interruption, is presented in Table 13. Aiming to develop an interruption schedule for uncertain loads without interrupting a specific device or set of devices frequently, this study limited the number of interruptions for each device in the mathematical model by adding an appropriate constraint. The considered interruptible devices were grouped into three major categories: residential, commercial, and industrial. Devices in the residential area have small loads and short durations, while industrial

devices have significantly larger capacities and longer durations. Commercial devices have slightly larger capacities and lower operational durations than those of residential devices. It should be noted that the last column of Table 13 shows whether a device type is interruptible. Non-interruptible devices such as dryers and washing machines are not used in the GA_{SILP}.

The results of the proposed simulation optimization framework are described in detail in the following subsection.

5.3.1. Results and Discussion of GA_{SILP}

Variation in devices' energy consumption may lead to different solutions for the proposed SILP. To overcome the issue of day-ahead scheduling of ILs, the proposed simulation and optimization framework was used to schedule uncertain ILs. In order to increase the solution quality and computational efficiency, the parameter values for the experiment (mutation rate, GA_{SILP} iterations, etc.) were obtained after preliminary experiments using the framework. During these experiments, an initial population of 210 feasible solutions was generated to start the genetic algorithm (GA_{SILP}). Solution performances were then evaluated based on the GA_{SILP}'s performance function, depending on the simulated capacities and results of the complete ranking OCBA.

Table 13: Summary of devices and load information for simulation and optimization framework

Device Types	Number of Devices	Max. Interruption	Base Device loads $E(C_k)$	Interruptible or not
Residential devices				
Dryer	189	-	1.2	No
Dishwasher	288	58	0.7	Yes
Washing Machine	268	-	0.5	No
Oven	279	56	1.3	Yes
Iron	340	68	1	Yes
Vacuum Cleaner	158	32	0.4	Yes
Fan	288	58	0.2	Yes
Lights	406	82	0.2	No
Water Heater	48	10	0.48	Yes
Desktop Computer	59	11	0.4	Yes
Hair Dryer	58	-	1.5	No
Sink Waste Disposal	66	15	0.45	Yes
Frying Pan	101	-	1.1	No
Coffee Maker	56	17	0.8	Yes
Total	2604	-	-	-
Commercial Devices				
Water Dispenser	156	30	2.5	Yes
Dryer	117	-	3.5	No
Kettle	123	24	3	Yes
Oven	77	15	5	Yes
Coffee Maker	99	20	2	Yes
Fan/AC	93	19	3.5	Yes
Air Conditioner	56	11	4	Yes
Lights	87	17	2	No
Total	808	-	-	-
Industrial Devices				
Water Heater	39	8	12.5	Yes
Welding Machine	35	7	25	Yes
Fan/AC	16	3	30	Yes
Arc Furnace	8	-	50	No
Induction Motor	5	1	100	Yes
DC Motor	6	-	150	No
Total	109	-	-	-

Here, device energy consumption was generated via normal distributions with mean (μ) equal to the expected value of device capacities (Table 13), and variance (σ^2) equal to $\mu/6$. The initial number of replications, additional replication budget, and total replication budget were set to 10 (n_0), 200 (Δ), and 10,000 (T), respectively. Once solutions were ranked, the top m (10) solutions were kept for the next iteration of the GA$_{SILP}$. In order to obtain $200\ (= 210 - 10)$ new solutions, 10 feasible solutions were generated randomly to add diversification to the solutions and avoid local optima. The remaining 190 solutions were generated by applying the crossover operator over all pairs of the 10 top-ranked solutions and 10 random solutions ($\binom{10+10}{2} = 190$). The mutation operator for the considered problem (p_{mu}) was set as 0.1 after assessing the initial experiments. Finally, the framework stopped operations with 200 generations of the GA$_{SILP}$ (200 iterations). The convergence plot of the GA$_{SILP}$ is illustrated in Fig. 23. The performances of the obtained solutions changed minimally after 60 iterations and seemed to be very close to each other. Consequently, variation in device energy consumption is the only source of variation among the solutions' performance after 60 iterations.

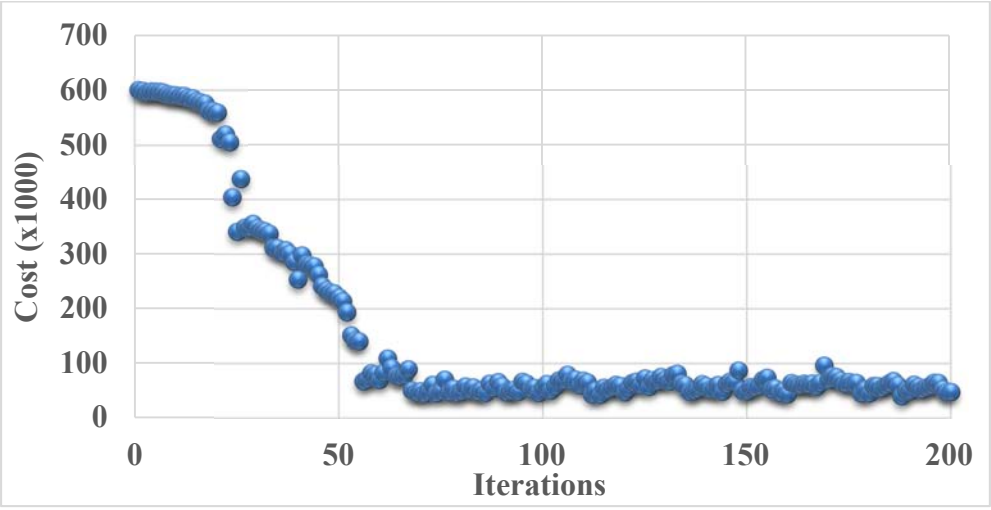

Fig. 23: Convergence plot of GA$_{SILP}$

5.3.2. Performance Evaluation of the Proposed Framework

This subsection describes the conducted comparison of the proposed simulation and optimization framework with relaxed deterministic optimization, random search, simulated annealing (SA), and the optimal case, which is unrealistic due to the predictive nature of day-ahead DR programs. In order to evaluate the efficiency of the obtained solutions compared to the relaxed deterministic optimization method, the SILP was relaxed using the expected value of $C_k^{\pm}$ ($\mu = E(C_k^{\pm})$) and optimized with an optimization approach. In other words, the SILP was optimized considering deterministic values for device loads ($E(C_k^{\pm})$ for device loads). The relaxed forms of (52) and (53) can be written as:

$$\min E\big(f(x)\big) = \min E\left(\sum_{k=1}^{N}\sum_{t=1}^{24} x_{kt}\ .R_k\ .\ C_k^{\pm}\right) \equiv \tag{52}$$

$$\min\ \sum_{k=1}^{N}\sum_{t=1}^{24} x_{kt}\ .R_k\ .\ E(C_k^{\pm})$$

$$E\left(\sum_{k=1}^{N}(f_{kt} - x_{kt})\cdot C_k^{\pm}\right) \geq E(D_t) \equiv \sum_{k=1}^{N}\big(f_{kt} - x_{kt}\big)\cdot E\big(C_k^{\pm}\big) \geq D_t \tag{53}$$

After obtaining the optimal schedule of the relaxed deterministic optimization problem, heuristic-based algorithms such as random search and SA were further optimized to find a near-optimal solution. These were compared to the proposed simulation optimization framework for efficiency purposes.

To compare the resulting scheduling of the proposed framework with the above algorithms, the energy load of each device was simulated with two different distributions, (N(E($C_k^{\pm}$), $E(C_k^{\pm})$/3) and N(E($C_k^{\pm}$), $E(C_k^{\pm})$/6), in 200 iterations for each distribution. The schedules obtained from the proposed framework were benchmarked against those obtained from the relaxed deterministic optimization, random search, and SA in terms of feasibility and average cost (200 device capacities for each), as summarized in Table 10.

The scheduling from the proposed simulation and optimization framework resulted in 80.5% and 64.5% feasible solutions for (N(E($C_k^{\pm}$), $E(C_k^{\pm})/3$) and N(E($C_k^{\pm}$), $E(C_k^{\pm})/6$); resulted in 21% and 12.5% feasible solutions in the relaxed deterministic optimization, 55% and 25% in the random search, and 25.5% and 17.5% in the SA algorithms. As mentioned previously, a feasible solution is a solution that does not exceed the desired load curve at any point. The comparison in Table 10 of the percentage of feasible solutions among the different algorithms reveals that the proposed framework reaches the highest percentage of feasibility with at least 30% more feasibility than the second-best algorithm (random search). Although the average total cost in relaxed deterministic optimization is lower than the proposed framework, it is important to point out that 52% and 59.5% higher feasibility was obtained in the proposed simulation and optimization framework (compared to the relaxed deterministic approach) by increasing the average cost slightly by 6.9% and 9.09%. Furthermore, high rates of infeasibility and unsatisfied demand in the relaxed deterministic optimization results may lead to a quite high cost in the case of energy instability or blackout in the considered system. Table 10 also indicates that there is a negative correlation between variance and feasibility percentage, where increasing the variance from $E(C_k^{\pm})/6$ to $E(C_k^{\pm})/3$ decreases the feasibility percentage and increases the cost.

Demand side management programs are commonly implemented a day ahead of time, and advance notices are used to notify participants. In this case, it is impossible to forecast the exact energy consumption of devices. However, at the end of a 24-hour period, the energy consumption of each device is known and can be used to evaluate the efficiency of the proposed framework. In the last row of Table 14, the results of the proposed

framework are compared to optimal scheduling for 200 sets of simulated demands. The average cost in the proposed framework has a quite promising performance with 88.21% and 88.47% of optimal costs for different variances. As mentioned previously, in a day-ahead DR with uncertain device loads, an optimal solution cannot be reached because of uncertain demands. As a result, device loads were only assumed to be known (called an optimal case) where optimal solutions and the ILM framework were compared to show the efficiency of the proposed framework.

Table 14: Comparison of the proposed ILM framework with relaxed deterministic optimization, random search, simulated annealing, and optimal case

	Demand mean (μ_k)	**Demand Variance (σ^2)**	**% of feasible solutions**	**Average of total cost**
Proposed framework	$E(C_k)$	$E(C_k)/6$	80.5% (161/200)	125,595
		$E(C_k)/3$	64.5% (129/200)	123,995
Relaxed deterministic optimization	$E(C_k)$	$E(C_k)/6$	21% (42/200)	115,123
		$E(C_k)/3$	12.5% (25/200)	115,949
Random search	$E(C_k)$	$E(C_k)/6$	55% (110/200)	127,333
		$E(C_k)/3$	25% (50/200)	124,213
Simulated annealing	$E(C_k)$	$E(C_k)/6$	25.5% (51/200)	129,776
		$E(C_k)/3$	17.5% (35/200)	124,505
Optimal case (unrealistic)	$E(C_k)$	$E(C_k)/6$	-	112,603
		$E(C_k)/3$	-	112,518

5.3.3. Final Scheduling of ILs

Fig. 24 illustrates the resulting load curve obtained as a result of the schedule produced by the proposed ILM framework compared to that obtained from the deterministic optimization; optimal loads for the 6 hours with highest demand are also shown. In Fig. 24, values of 4 and 10 on the time axis represent 10:00 A.M. and 4:00 P.M., respectively. The comparison of the desired demand (gray line) and the average ILM framework load (orange line) reveals that the proposed framework manages to satisfy the required curtailment for all 6-hour periods, while the average loads in the deterministic optimization

approach exceeds the desired demand for 2 hours, including during the 11:00 A.M.–1:00 P.M. time period. Since satisfaction of the required curtailment improves grid sustainability and reduces the need to construct under-utilized energy facilities with enormous costs, the proposed ILM framework succeeds in reducing the peak load demand of the smart grid.

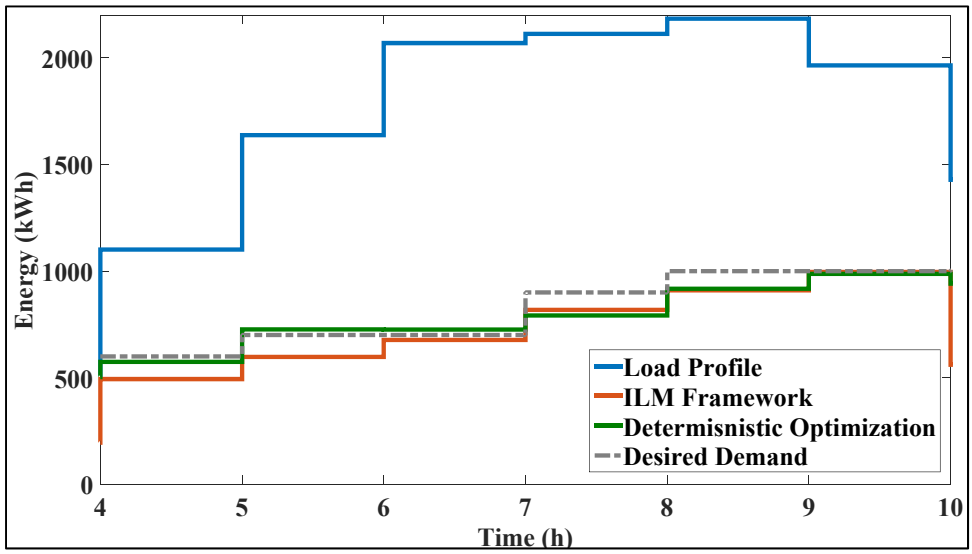

Fig. 24: Desired demand, deterministic optimization, and proposed ILM framework load curves

Chapter 6

Conclusions and Future Work

This study has proposed two simulation and optimization frameworks (F1 & F2) to determine (near-)optimal 24-hour-ahead load scheduling for loads and buildings in smart grids. This doctoral research provides simulation and optimization tools for energy providers and third-party aggregators to schedule energy loads in smart grids to satisfy desired load demand. The main capability of the proposed frameworks is the consideration of deterministic and stochastic loads in two separate frameworks to provide flexibility for users. The aim of this research was to examine how the invention of smart meters (ECCs) and integration of multiple renewable energies can satisfy customer loads in day-ahead scheduling.

In particular, the first part of this study proposed a DDD-MOM for the operation planning of smart grids with simplified assumptions. This DDD-MOM served as an introductory effort to proposing the simulation and optimization frameworks (F1 & F2) for DSM implementation in smart grids. The proposed model consisted of three main modules: data simulation, bi-objective optimization, and RTDM. First, the simulation module took historical data and mimicked the behavior of components of the smart grid, considering uncertainties associated with power generation from distributed energy resources and load demand. In the next step, the results of the simulation and linearized form of the quadratic cost and emission functions of diesel generators were imported into the bi-objective optimization model. Then, the bi-objective optimization model was solved using an ϵ-constraint method to obtain the best compromise solution. In the last module, the rule-based RTDM modified the solution obtained from the optimization module to finalize the

operation plan based on dynamic data from the smart grid to satisfy all operational constraints. The performance of the proposed approach was demonstrated through a synthetic smart grid that included solar panels, wind turbines, and four types of diesel generators. The results show that a DDD-MOM can provide a real-time hourly operation plan for a smart grid without harming the feasibility and optimal solution obtained from an optimization model. The DDD-MOM proposed in this study was designed in a generic manner and illustrates how renewable energies can be utilized in smart grids.

In the second part of this study, a deterministic multi-objective optimization framework for load shifting in smart grids is proposed, which considers three objective functions: cost and emission minimization and customer satisfaction. The proposed multi-objective optimization framework was composed of four main components: (1) a forecasting model to obtain a 24-hour-ahead energy load, (2) a load shifting DSM program to reduce the energy load during peak demand, (3) a PWL approximation method to linearize the non-linear objective functions and constraints, and (4) an advanced ϵ-constraint multi-objective optimization method to efficiently acquire Pareto frontier solutions. This study also presents an advanced ϵ-constraint method to acquire a Pareto frontier solution set with a higher percentage of non-dominated solutions (72% more) in less computational time than the traditional ϵ-constraint. The novelty of this part of the research lies in the consideration of different stakeholders' objectives and the improvement of the traditional ϵ-constraint by proposing an advanced ϵ-constraint method.

Finally, the third part of this study proposed an evolutionary simulation optimization framework for ILM in smart grids that attempts to minimize the total interruption cost while considering uncertainty among devices' energy consumption. The proposed ILM

framework comprises three integrated components: a genetic algorithm that progressively improves existing scenarios or discovers new scenarios for interruption, a simulation model that simulates the performance of selected scenarios, and a simulation design-ranking algorithm that optimizes the allocation of simulation replications and identifies the top $\boldsymbol{m}$ best scenarios. The results from a smart grid case study reveal that scheduling ILs with noisy device loads using the ILM framework leads to substantially more feasible solutions than the deterministic approach, random search, and SA. Moreover, the proposed simulation optimization framework generates schedules with accuracies of 88.21% and 88.47% in two datasets compared to optimal solutions.

Future avenues for this work include conducting a dynamic data-driven DSM for the resilient operation of smart grids. With the rise of the smart city concept using information and communication technologies (ICTs) for communication between citizens and suppliers, DSM programs can reduce power outages in an efficient manner. While smart grids and DSM programs promise great advantages, an electric power grid is made up of many geographically dispersed components, and natural disasters such as hurricanes or storms pose major challenges for reliable energy supply. Such disasters can happen with little or no warning, leaving hundreds or even thousands of people without electrical coverage, medical services, potable water, sanitation, and communications for up to several weeks. For instance, the 2004 hurricane season ravaged the state of Florida with four major hurricanes in a 6-week timeframe. In emergency conditions, using a fast-response DSM program that has the flexibility to update data based on the most recent weather forecast, energy generation, and load demand information is essential. Therefore, future efforts will be made to present a dynamic data-driven DSM framework to determine (near-)optimal

scheduling of energy loads to prevent energy shortages during emergency conditions. The future study is inspired by the dynamic data-driven application systems (DDDAS) paradigm established by [63, 64] that has the ability to create a symbiotic feedback loop for the incorporation of dynamic data in an application system (i.e., the load scheduling optimization model in this study) and the ability to steer the measurement process of the real system (i.e., the response of the real system in this study). A schematic figure of the considered framework in case of emergency is shown in Fig. 25.

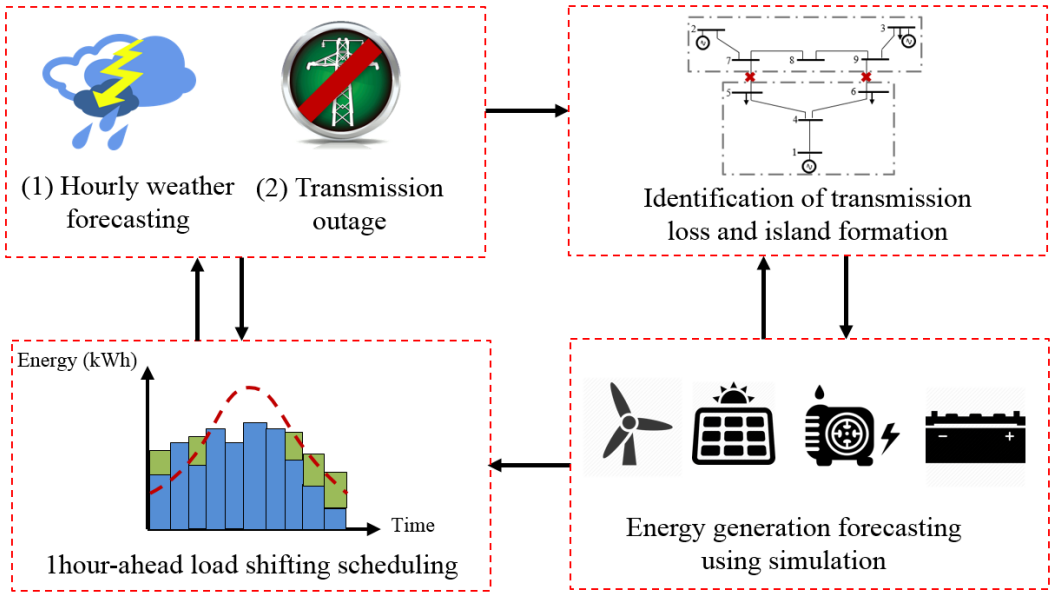

Fig. 25: DDDAS-based framework for DSM during emergency conditions

Once a framework for the resilient operation of a smart grid is created, future studies may extend the scope of the load shifting program to integrate ILM and load shifting simultaneously. Furthermore, the optimization and simulation modules can be integrated and operated in the Anylogic software for ease of application.

References

1. Gellings, C.W., & Chamberlin, J. H., *Demand-side management.* 1988.

2. Palensky, P. and D. Dietrich, *Demand side management: Demand response, intelligent energy systems, and smart loads.* IEEE transactions on industrial informatics, 2011. **7**(3): p. 381-388.

3. Saad, W., et al., *Game-theoretic methods for the smart grid: An overview of microgrid systems, demand-side management, and smart grid communications.* IEEE Signal Processing Magazine, 2012. **29**(5): p. 86-105.

4. Strbac, G., *Demand side management: Benefits and challenges.* Energy policy, 2008. **36**(12): p. 4419-4426.

5. Wang, B., Y. Li, and C. Gao, *Demand side management outlook under smart grid infrastructure.* Automation of Electric Power Systems, 2009. **20**: p. 17-22.

6. Boshell, F. and O. Veloza. *Review of developed demand side management programs including different concepts and their results*. in *Transmission and Distribution Conference and Exposition: Latin America, 2008 IEEE/PES*. 2008. IEEE.

7. Ming-jun, W., *Load management and demand side management in electricity market environment [J]*. Power System Technology, 2005. **5**: p. 000.

8. Mohsenian-Rad, A.-H., et al., *Autonomous demand-side management based on game-theoretic energy consumption scheduling for the future smart grid.* IEEE transactions on Smart Grid, 2010. **1**(3): p. 320-331.

9. Logenthiran, T., D. Srinivasan, and T.Z. Shun, *Demand side management in smart grid using heuristic optimization.* IEEE transactions on smart grid, 2012. **3**(3): p. 1244-1252.

10. Gao, D.-c. and Y. Sun, *A GA-based coordinated demand response control for building group level peak demand limiting with benefits to grid power balance.* Energy and Buildings, 2016. **110**: p. 31-40.

11. Mišák, S., et al., *A heuristic approach to Active Demand Side Management in Off-Grid systems operated in a Smart-Grid environment.* Energy and buildings, 2015. **96**: p. 272-284.

12. Bashash, S. and H.K. Fathy. *Robust demand-side plug-in electric vehicle load control for renewable energy management*. in *American Control Conference (ACC), 2011*. 2011. IEEE.

13. Li, Z. and T. Yao. *Renewable energy basing on smart grid*. in *Wireless Communications Networking and Mobile Computing (WiCOM), 2010 6th International Conference on*. 2010. IEEE.

14. Forte, V.J. *Smart grid at national grid*. in *Innovative Smart Grid Technologies (ISGT), 2010*. 2010. IEEE.

15. Shivaharinathan, B., et al., *Review of demand side management of optimal scheduling of future loads [J]*. International Journal of Electrical Transformation and Restructuring, 2016. **1**(1): p. 64-67.

16. Mohsenian-Rad, A.-H. and A. Leon-Garcia, *Optimal residential load control with price prediction in real-time electricity pricing environments.* IEEE transactions on Smart Grid, 2010. **1**(2): p. 120-133.

17. Motegi, N., et al., *Introduction to commercial building control strategies and techniques for demand response.* Lawrence Berkeley National Laboratory LBNL-59975, 2007.

18. Potter, C.W., A. Archambault, and K. Westrick. *Building a smarter smart grid through better renewable energy information*. in *Power Systems Conference and Exposition, 2009. PSCE'09. IEEE/PES*. 2009. IEEE.

19. Chiu, A., et al., *Framework for integrated demand response (DR) and distributed energy resources (DER) models.* NAESB & UCAIug. September, 2009.

20. Mohagheghi, S., et al. *Demand response architecture: Integration into the distribution management system*. in *Smart Grid Communications (SmartGridComm), 2010 First IEEE International Conference on*. 2010. IEEE.

21. Tsoukalas, L. and R. Gao. *From smart grids to an energy internet: Assumptions, architectures and requirements*. in *Electric Utility Deregulation and Restructuring and Power Technologies, 2008. DRPT 2008. Third International Conference on*. 2008. IEEE.

22. Bhattacharya, K., M. Bollen, and J.E. Daalder, *Operation of restructured power systems*. 2012: Springer Science & Business Media.

23. Siano, P., *Demand response and smart grids—A survey.* Renewable and Sustainable Energy Reviews, 2014. **30**: p. 461-478.

24. Herter, K., P. McAuliffe, and A. Rosenfeld, *An exploratory analysis of California residential customer response to critical peak pricing of electricity.* Energy, 2007. **32**(1): p. 25-34.

25. Behrangrad, M., H. Sugihara, and T. Funaki. *Analyzing the system effects of optimal demand response utilization for reserve procurement and peak clipping*. in *Power and Energy Society General Meeting, 2010 IEEE*. 2010. IEEE.

26. Lim, K.Y., *User interface and development of future active network management system for microgrid*. 2013, UTAR.

27. Huang, K.-Y., H.-C. Chin, and Y.-C. Huang, *A model reference adaptive control strategy for interruptible load management.* IEEE Transactions on Power Systems, 2004. **19**(1): p. 683-689.

28. Shen, J., C. Jiang, and B. Li, *Controllable load management approaches in smart grids.* Energies, 2015. **8**(10): p. 11187-11202.

29. Ashok, S. and R. Banerjee, *An optimization mode for industrial load management.* IEEE Transactions on Power Systems, 2001. **16**(4): p. 879-884.

30. Vandael, S., et al., *A scalable three-step approach for demand side management of plug-in hybrid vehicles.* IEEE Transactions on Smart Grid, 2013. **4**(2): p. 720-728.

31. Arteconi, A., N.J. Hewitt, and F. Polonara, *Domestic demand-side management (DSM): Role of heat pumps and thermal energy storage (TES) systems.* Applied thermal engineering, 2013. **51**(1): p. 155-165.

32. Graditi, G., et al., *Heuristic-based shiftable loads optimal management in smart micro-grids.* IEEE Transactions on Industrial Informatics, 2015. **11**(1): p. 271-280.

33. Tasdighi, M., H. Ghasemi, and A. Rahimi-Kian, *Residential microgrid scheduling based on smart meters data and temperature dependent thermal load modeling.* IEEE Transactions on Smart Grid, 2014. **5**(1): p. 349-357.

34. Thanos, A.E., et al., *System of systems modeling and simulation for microgrids using DDDAMS.* Modeling and Simulation Support for System of Systems Engineering Applications, 2015: p. 337.

35. Parker, D.S., *Research highlights from a large scale residential monitoring study in a hot climate.* Energy and Buildings, 2003. **35**(9): p. 863-876.

36. Yu, D.C., T.C. Nguyen, and P. Haddawy, *Bayesian network model for reliability assessment of power systems.* IEEE Transactions on Power Systems, 1999. **14**(2): p. 426-432.

37. Tong, W., *Wind power generation and wind turbine design*. 2010: WIT press.

38. Finn, P. and C. Fitzpatrick, *Demand side management of industrial electricity consumption: promoting the use of renewable energy through real-time pricing.* Applied Energy, 2014. **113**: p. 11-21.

39. Kass, R.E. and A.E. Raftery, *Bayes factors.* Journal of the american statistical association, 1995. **90**(430): p. 773-795.

40. Raftery, A.E., *Choosing models for cross-classifications.* American sociological review, 1986. **51**(1): p. 145-146.

41. Sato, T., Y. Takano, and R. Miyashiro, *Piecewise-linear approximation for feature subset selection in a sequential logit model.* Journal of the Operations Research Society of Japan, 2017. **60**(1): p. 1-14.

42. Mavrotas, G., *Effective implementation of the ε-constraint method in multi-objective mathematical programming problems.* Applied mathematics and computation, 2009. **213**(2): p. 455-465.

43. Atwa, Y., et al., *Optimal renewable resources mix for distribution system energy loss minimization.* IEEE Transactions on Power Systems, 2010. **25**(1): p. 360-370.

44. (FAWN), F.A.W.N., *Yearly csv data*. 2013, University of Florida

45. Setämaa-Kärkkäinen, A., K. Miettinen, and J. Vuori, *Best compromise solution for a new multiobjective scheduling problem.* Computers & operations research, 2006. **33**(8): p. 2353-2368.

46. Amjady, N., *Short-term bus load forecasting of power systems by a new hybrid method.* IEEE Transactions on Power Systems, 2007. **22**(1): p. 333-341.

47. Hernandez, L., et al., *Short-term load forecasting for microgrids based on artificial neural networks.* Energies, 2013. **6**(3): p. 1385-1408.

48. Kanchev, H., et al., *Energy management and operational planning of a microgrid with a PV-based active generator for smart grid applications.* IEEE transactions on industrial electronics, 2011. **58**(10): p. 4583-4592.

49. Taylor, J.W., *An evaluation of methods for very short-term load forecasting using minute-by-minute British data.* International Journal of Forecasting, 2008. **24**(4): p. 645-658.

50. Taylor, J.W. and P.E. McSharry, *Short-term load forecasting methods: An evaluation based on european data.* IEEE Transactions on Power Systems, 2007. **22**(4): p. 2213-2219.

51. Thanos, A.E., et al., *Dynamic data driven adaptive simulation framework for automated control in microgrids.* IEEE Transactions on Smart Grid, 2017. **8**(1): p. 209-218.

52. Abido, M., *Multiobjective particle swarm optimization for environmental/economic dispatch problem.* Electric Power Systems Research, 2009. **79**(7): p. 1105-1113.

53. Rau, R.T., *Piecewise Linear Approximation.* Geometric Modeling: Theory and Practice: The State of the Art, 2012: p. 335.

54. Holland, J.H., *Adaptation in natural and artificial systems: an introductory analysis with applications to biology, control, and artificial intelligence*. 1992: MIT press.

55. Damgacioglu, H., et al., *A genetic algorithm for the uncapacitated single allocation planar hub location problem.* Computers & Operations Research, 2015. **62**: p. 224-236.

56. Bastani, M., et al. *Efficient design selection in microgrid simulations*. in *Simulation Conference (WSC), 2014 Winter*. 2014. IEEE.

57. Chen, C.-h. and L.H. Lee, *Stochastic simulation optimization: an optimal computing budget allocation*. Vol. 1. 2011: World scientific.

58. Chen, C.-H., et al., *Optimal budget allocation for discrete-event simulation experiments.* IIE Transactions, 2009. **42**(1): p. 60-70.

59. Goldsman, D. and B.L. Nelson. *Ranking, selection and multiple comparisons in computer simulation*. in *Simulation Conference Proceedings, 1994. Winter*. 1994. IEEE.

60. He, D., et al., *Simulation optimization using the cross-entropy method with optimal computing budget allocation.* ACM Transactions on Modeling and Computer Simulation (TOMACS), 2010. **20**(1): p. 4.

61. Lee, L.H., et al., *A review of optimal computing budget allocation algorithms for simulation optimization problem.* International Journal of Operations Research, 2010. **7**(2): p. 19-31.

62. Xiao, H., L.H. Lee, and K.M. Ng, *Optimal computing budget allocation for complete ranking.* IEEE Transactions on Automation Science and Engineering, 2014. **11**(2): p. 516-524.

63. Darema, F., *Dynamic data driven application systems.* Internet Process Coordination, 2002: p. 149.

64. Darema, F., *Dynamic data driven applications systems: A new paradigm for application simulations and measurements.* Computational Science-ICCS 2004, 2004: p. 662-669.

Appendix I: Multi-objective Optimization AMPL Code

```
option solver cplexamp;

option display_round 6;

model "C:\Users\mehradba\Desktop\Mehrad Backup Oct- 2015\Mehrad Bastani\DSM-Optimization\Code-Final\code_v7.txt";

table bbb IN "ODBC" "C:\Users\mehradba\Desktop\Mehrad Backup Oct- 2015\Mehrad Bastani\DSM-Optimization\Code-Final\hourbaseddata.xls":
        HOUR <- [HOUR], D, RS;
read table bbb;

table forecast IN "ODBC" "C:\Users\mehradba\Desktop\Mehrad Backup Oct-2015\Mehrad Bastani\DSM-Optimization\Code-Final\fdata.xls":
        BUILD <- [i ~ BUILD], {j in HOUR} <F[i,j] ~ (j)> ;
read table forecast;

table aaa IN "ODBC" "C:\Users\mehradba\Desktop\Mehrad Backup Oct- 2015\Mehrad Bastani\DSM-Optimization\Code-Final\param1.xls":
        GEN <- [GEN], PGmin, CS, CI, EI;
read table aaa;

table f IN "ODBC" "C:\Users\mehradba\Desktop\Mehrad Backup Oct- 2015\Mehrad Bastani\DSM-Optimization\Code-Final\param2.xls":
        BUILD <- [i ~ BUILD], UI;
read table f;

table bb IN "ODBC" "C:\Users\mehradba\Desktop\Mehrad Backup Oct- 2015\Mehrad Bastani\DSM-Optimization\Code-Final\param2.xls":
        SEG <- [k ~ SEG], {j in GEN} <ES[j, k] ~ (j)> ;
read table bb;

table ccc IN "ODBC" "C:\Users\mehradba\Desktop\Mehrad Backup Oct- 2015\Mehrad Bastani\DSM-Optimization\Code-Final\param2.xls":
        [i ~ BUILD], {k in SEG} < US[i,k] ~ (k) >;
read table ccc;

table ddd IN "ODBC" "C:\Users\mehradba\Desktop\Mehrad Backup Oct- 2015\Mehrad Bastani\DSM-Optimization\Code-Final\param2.xls":
        [j ~ GEN], {r in 1..4} < GR[j,r] ~ (r) >;
read table ddd;

table eee IN "ODBC" "C:\Users\mehradba\Desktop\Mehrad Backup Oct- 2015\Mehrad Bastani\DSM-Optimization\Code-Final\param2.xls":
        [i ~ BUILD], {r in 1..4} < UR[i,r] ~ (r) >;
read table eee;
```

```
option solver_msg 0;

# Primary Objective #

problem initial1: Total_Cost, Required_Curtailment, generation_limit, utility_st, shifting_ps, gen_seg, utility_seg, seg, seg1, s, sp, g, gs, u, us, v;

solve initial1;

# Primary Objective #

problem initial2: emission, Required_Curtailment, generation_limit, utility_st, shifting_ps, gen_seg, utility_seg, seg, seg1, s, sp, g, gs, u, us, v;

solve initial2;

# Primary Objective #

problem initial3: utility, Required_Curtailment, generation_limit, utility_st, shifting_ps, gen_seg, utility_seg, seg, seg1, s, sp, g, gs, u, us, v;

solve initial3;

# CONSTRUCTING PAYOFF TABLE #

param tempRHS2;

param tempLHS3;

param tempLHS2;

let TC:=0;

printf "------------------------------\n" > out_DSM.txt;

printf "Payoff Table\n" > out_DSM.txt ;

printf "O/O  \t obj1 \t \t obj2 \t \t obj3 \n" > out_DSM.txt;

# Primary Objective #

problem initial1: Total_Cost, Required_Curtailment, generation_limit, shifting_ps, gen_seg, gen_seg2, utility_seg, seg, seg1, seg2, shift_cap, s, sp, g, gs, us, v, obj2_lb, obj3_lb;

solve initial1;
```

```
printf "obj1 \t %5.2f \t %6.2f \t %6.2f \t %6.2f \n", Total_Cost, obj2_lb.body, obj3_lb.body,
_solve_elapsed_time > out_DSM.txt;

let tempRHS2:=obj2_lb.body;

let tempLHS3:=obj3_lb.body;

# Second Objective #

problem initial2: emission, Required_Curtailment, generation_limit, shifting_ps, gen_seg,

gen_seg2, utility_seg, seg, seg1, seg2, shift_cap, s, sp, g, gs, us, v, obj2_lb, obj3_lb;

solve initial2;

printf "obj2 \t %5.2f \t %6.2f \t %6.2f \t %6.2f \n", obj1_lb.body, emission, obj3_lb.body,
_solve_elapsed_time > out_DSM.txt;

let LHS2:=emission;

let tempLHS2:=emission;

let tempLHS3:=min(tempLHS3, obj3_lb.body) ;

# Third Objective #

problem initial3: utility, Required_Curtailment, generation_limit, shifting_ps, gen_seg,

gen_seg2, utility_seg, seg, seg1, seg2, shift_cap, s, sp, g, gs, us, v, obj2_lb, obj3_lb;

solve initial3;

printf "obj3 \t %5.2f \t %6.2f \t %6.2f \t %6.2f \n", obj1_lb.body, obj2_lb.body, utility,
_solve_elapsed_time  > out_DSM.txt ;

let RHS3:=utility;

let tempRHS2:=max(tempRHS2, obj2_lb.body) ;

printf "------------------------------\n" > out_DSM.txt;

display LHS2, tempRHS2, tempLHS3, RHS3;

let LHS3:=tempLHS3;

let RHS2:=tempRHS2;
```

```
param beta;

param terminate;

param iteration1;

param iteration2;

param delta1;

param delta2;

let beta:=1;

let terminate:=0;

let iteration1:=0;

let iteration2:=0;

let delta1:=351.2;

let delta2:=0.025;

option cplex_options 'sensitivity';

problem main: Total_Cost, Required_Curtailment, generation_limit, shifting_ps, gen_seg,

gen_seg2, utility_seg, seg, seg1, seg2, shift_cap, s, sp, g, gs, us, v, obj2_ub, obj3_lb, obj2_lb, obj3_ub;

problem uproblem: utility, Required_Curtailment, generation_limit, shifting_ps, gen_seg,

gen_seg2, utility_seg, seg, seg1, seg2, shift_cap, s, sp, g, gs, us, v, obj1_lb, obj2_ub, obj2_lb;

problem eproblem: emission, Required_Curtailment, generation_limit, shifting_ps, gen_seg, gen_seg2, utility_seg, seg, seg1, seg2, shift_cap, s, sp, g, gs, us, v, obj1_lb;

#suffix down OUT;

#suffix current OUT;

#suffix up OUT;
```

```
##---Calculating first interval--
solve main;
display obj2_ub.body;
if obj2_ub.dual=0 then {
        let TC:=Total_Cost;
        solve eproblem;
        let RHS2:=emission;
}
else let RHS2:=obj2_ub.body;
printf "--------------------\n"> out_DSM.txt;
repeat while iteration1<100 {
        let LHS2:=tempLHS2+(iteration1 * delta1);
        let RHS2:=tempLHS2+((iteration1+1) * delta1);
        display LHS2, RHS2;
        repeat while iteration2<100 {
                let LHS3:=tempLHS3+iteration2*delta2;
                let RHS3:=tempLHS3+(iteration2+1)*delta2;
                display LHS3, RHS3;
                solve main;
                /*if solve_result <> "infeasible" then break;*/
                display Total_Cost, obj2_lb.body, obj3_lb.body;
                printf "solution %d \t %.8f \t %0.8f \t %0.8f \t %0.8f \n", iteration1,
Total_Cost, obj2_lb.body, obj3_lb.body, _solve_elapsed_time > out_DSM.txt;
                let iteration2:= iteration2+1;
                }
```

```
let iteration1:=iteration1+1;

};

solve main;

let LHS2:=obj2_ub.down;

display LHS2, RHS2;

if obj3_lb.dual=0 then {

let iteration:=iteration+1;

let TC:=Total_Cost;

solve uproblem;

printf "solution %d \t %.8f \t %0.8f \t %0.8f \t %0.8f \n", iteration, obj1_lb.body,
obj2_ub.body, utility, _solve_elapsed_time > out_DSM.txt;

if obj1_lb.dual<>0 then {

let iteration:=iteration+1;

display LHS2, RHS2;

let TC:=10000000;

solve uproblem;

printf "solution %d \t %.8f \t %0.8f \t %0.8f \t %0.8f \n", iteration, obj1_lb.body,
obj2_ub.body, utility, _solve_elapsed_time > out_DSM.txt;

}

else printf "solution %d \t %.8f \t %0.8f \t %0.8f \t %0.8f \n", iteration, Total_Cost,
obj2_ub.body, obj3_lb.body, _solve_elapsed_time > out_DSM.txt;

}

let RHS2:=LHS2-beta;

let LHS2:=tempLHS2;

if iteration>3000 then break;

if RHS2<tempLHS2 then break;
```

```
        let iteration:=iteration+1;
        };
printf "--------------------\n" > out_DSM.txt;*/
```

Appendix II: Comparison of Pareto Frontier Solutions

Pareto frontier solutions set obtained by traditional ϵ-constraint method							
Solution Number	**Cost**	**Emission**	**Customer Satisfaction**	**Solution Number**	**Cost**	**Emission**	**Customer Satisfaction**
1	548.59	5718.71	0.0157	22	555.65	1793.33	0.0157
2	549.37	4809.67	0.0157	23	556.57	1635.28	0.0157
3	549.39	5541.17	0.0443	24	556.66	1812.82	0.0443
4	550.02	5363.63	0.0443	25	556.82	5363.63	0.0730
5	550.08	4653.47	0.0157	26	557.33	5032.07	0.0730
6	550.48	4831.01	0.0443	27	557.55	4465.80	0.0730
7	550.59	3804.17	0.0157	28	558.55	4026.57	0.0773
8	550.77	3765.77	0.0157	29	559.45	769.28	0.0157
9	550.82	5186.09	0.0443	30	559.66	1457.74	0.0443
10	550.87	4475.93	0.0443	31	560.20	747.58	0.0157
11	551.51	4298.39	0.0443	32	560.46	1280.20	0.0443
12	551.57	3588.23	0.0157	33	560.60	3021.14	0.0730
13	552.05	3997.65	0.0443	34	560.93	962.73	0.0443
14	552.36	3410.69	0.0157	35	562.81	2345.45	0.0730
15	552.64	2798.74	0.0157	36	563.61	2015.73	0.0750
16	553.08	2700.53	0.0157	37	566.45	1457.74	0.0730
17	553.21	3233.15	0.0443	38	567.25	1280.20	0.0730
18	553.88	2522.99	0.0157	39	567.56	999.75	0.0730
19	554.10	2992.22	0.0197	40	599.36	570.04	-0.0704
20	554.10	2992.22	0.0443	41	664.35	392.50	-0.1565
21	555.44	2345.45	0.0157				

Pareto frontier solutions set obtained by advanced ϵ-constraint method							
Solution Number	**Cost**	**Emission**	**Customer Satisfaction**	**Solution Number**	**Cost**	**Emission**	**Customer Satisfaction**
1	548.59	5718.71	0.062	**305**	712.47	325.29	-0.188
2	548.59	5717.71	0.062	**306**	713.50	324.20	-0.189
3	548.87	5657.04	0.062	**307**	714.56	323.13	-0.190
4	549.37	4809.67	0.062	**308**	715.72	321.98	-0.191
5	549.38	4808.67	0.062	**309**	716.81	320.89	-0.192
6	549.65	4748.00	0.062	**310**	717.85	319.86	-0.193
7	550.59	3804.17	0.062	**311**	718.94	318.76	-0.194
8	550.60	3803.17	0.062	**312**	720.00	317.73	-0.195
9	551.79	3538.71	0.062	**313**	721.73	315.98	-0.189
10	552.06	3478.04	0.062	**314**	722.66	314.97	-0.190
11	552.64	2798.74	0.062	**315**	723.58	313.88	-0.234
12	552.64	2797.74	0.062	**316**	724.27	312.88	-0.238
13	553.66	2572.79	0.062	**317**	725.01	311.82	-0.243
14	553.93	2512.13	0.062	**318**	725.76	310.74	-0.248
15	553.94	2510.29	0.062	**319**	726.46	309.73	-0.253
16	553.95	2508.66	0.062	**320**	727.18	308.70	-0.258
17	553.97	2506.85	0.062	**321**	727.93	307.69	-0.262
18	553.98	2505.21	0.062	**322**	729.00	306.52	-0.262
19	554.00	2501.90	0.062	**323**	729.98	305.46	-0.263
20	554.04	2495.21	0.061	**324**	730.95	304.40	-0.264
21	554.07	2490.54	0.061	**325**	731.97	303.31	-0.264
22	554.11	2484.57	0.061	**326**	733.02	302.26	-0.267
23	554.14	2480.40	0.061	**327**	734.49	300.79	-0.272
24	554.17	2475.68	0.061	**328**	735.59	299.69	-0.276
25	554.20	2470.88	0.061	**329**	736.63	298.66	-0.279
26	554.22	2468.51	0.061	**330**	737.72	297.57	-0.283
27	554.23	2466.51	0.061	**331**	738.82	296.50	-0.287
28	554.25	2463.63	0.061	**332**	740.00	295.37	-0.264
29	554.27	2461.26	0.061	**333**	741.02	294.21	-0.265
30	554.28	2458.84	0.061	**334**	742.17	293.06	-0.269
31	554.30	2455.79	0.060	**335**	746.21	289.20	-0.286
32	554.32	2454.24	0.060	**336**	747.26	288.19	-0.291
33	554.35	2449.64	0.060	**337**	748.44	287.06	-0.296
34	554.38	2444.06	0.060	**338**	751.53	283.29	-0.271
35	554.40	2441.97	0.060	**339**	752.63	282.23	-0.276
36	554.41	2439.78	0.060	**340**	761.25	273.98	-0.314
37	554.42	2438.05	0.060	**341**	762.45	272.84	-0.322
38	554.43	2436.41	0.060	**342**	763.74	271.60	-0.332
39	554.44	2435.34	0.060	**343**	764.93	270.47	-0.341
40	554.46	2433.05	0.060	**344**	766.03	269.41	-0.350
41	554.47	2430.81	0.060	**345**	769.97	265.74	-0.373
42	554.48	2428.95	0.060	**346**	771.17	264.70	-0.375
43	554.52	2424.10	0.060	**347**	772.93	263.20	-0.383
44	554.54	2420.72	0.060	**348**	774.20	262.12	-0.389
45	554.55	2418.35	0.060	**349**	775.52	260.99	-0.398
46	554.56	2416.65	0.059	**350**	776.08	418.25	-0.009
47	554.59	2413.62	0.059	**351**	776.81	259.89	-0.407
48	554.60	2410.84	0.059	**352**	777.35	417.15	-0.010
49	554.63	2406.97	0.059	**353**	778.86	258.14	-0.423
50	554.66	2402.26	0.059	**354**	779.28	429.62	0.000

51	554.68	2399.76	0.059	**355**	780.76	439.48	0.008
52	554.72	2393.12	0.059	**356**	781.73	424.77	-0.004
53	554.74	2390.73	0.059	**357**	781.80	411.15	-0.015
54	554.75	2388.86	0.059	**358**	782.11	438.39	0.007
55	554.76	2386.94	0.059	**359**	782.55	437.36	0.006
56	554.78	2383.99	0.059	**360**	782.75	410.11	-0.015
57	554.80	2381.34	0.059	**361**	783.60	409.00	-0.016
58	554.82	2378.53	0.058	**362**	783.61	454.62	0.018
59	554.83	2377.06	0.058	**363**	783.70	423.68	-0.005
60	554.85	2373.65	0.058	**364**	783.71	256.26	-0.391
61	554.87	2370.06	0.058	**365**	783.95	436.26	0.005
62	554.90	2368.08	0.058	**366**	784.37	407.07	-0.018
63	555.00	2364.07	0.058	**367**	784.98	421.77	-0.006
64	555.16	2357.41	0.058	**368**	785.01	255.19	-0.399
65	555.26	2352.94	0.058	**369**	785.14	453.33	0.017
66	555.39	2347.40	0.058	**370**	785.35	420.70	-0.007
67	555.46	2344.46	0.058	**371**	785.61	434.45	0.004
68	555.65	1793.33	0.061	**372**	785.94	403.84	-0.021
69	555.66	1792.33	0.061	**373**	786.14	254.19	-0.408
70	555.80	1761.97	0.061	**374**	786.17	419.67	-0.008
71	555.83	1753.40	0.061	**375**	786.36	452.23	0.017
72	555.86	1748.81	0.061	**376**	786.40	405.14	-0.020
73	555.89	1741.67	0.061	**377**	786.57	433.41	0.003
74	555.90	1738.48	0.061	**378**	786.74	352.00	-0.068
75	555.93	1731.66	0.061	**379**	787.05	401.34	-0.023
76	555.94	1730.50	0.061	**380**	787.19	402.61	-0.022
77	555.95	1729.01	0.061	**381**	787.45	253.07	-0.417
78	555.96	1727.44	0.061	**382**	787.56	432.33	0.002
79	555.97	1725.64	0.061	**383**	787.82	350.98	-0.069
80	556.01	1720.34	0.061	**384**	787.86	450.94	0.016
81	556.02	1718.70	0.061	**385**	788.54	349.71	-0.070
82	556.04	1715.63	0.060	**386**	788.76	251.96	-0.436
83	556.08	1709.51	0.060	**387**	788.81	399.55	-0.024
84	556.11	1704.62	0.060	**388**	788.94	430.82	0.001
85	556.13	1701.49	0.060	**389**	789.10	348.71	-0.071
86	556.15	1699.43	0.060	**390**	789.11	548.63	0.075
87	556.18	1694.42	0.060	**391**	789.19	449.84	0.015
88	556.20	1690.94	0.060	**392**	789.70	547.27	0.075
89	556.22	1688.77	0.060	**393**	789.72	448.61	0.014
90	556.24	1686.14	0.060	**394**	789.85	347.39	-0.073
91	556.26	1682.02	0.060	**395**	790.15	398.41	-0.025
92	556.29	1677.75	0.060	**396**	790.23	546.08	0.074
93	556.30	1676.31	0.059	**397**	791.18	543.91	0.073
94	556.33	1672.37	0.059	**398**	791.34	447.38	0.013
95	556.34	1670.79	0.059	**399**	792.30	446.33	0.012
96	556.35	1668.63	0.059	**400**	792.35	393.53	-0.030
97	556.36	1667.50	0.059	**401**	792.74	250.86	-0.390
98	556.40	1662.09	0.059	**402**	793.32	443.92	0.010
99	556.43	1657.24	0.059	**403**	793.52	392.50	-0.030
100	556.45	1653.66	0.059	**404**	793.93	249.84	-0.398
101	556.48	1650.26	0.059	**405**	794.74	464.71	0.025
102	556.48	1649.20	0.059	**406**	795.09	390.64	-0.032
103	556.49	1647.26	0.059	**407**	795.16	248.79	-0.407

104	556.53	1641.53	0.059	**408**	795.55	533.95	0.068
105	556.56	1636.97	0.058	**409**	795.97	532.77	0.067
106	556.58	1634.31	0.058	**410**	796.03	372.53	-0.048
107	556.59	1632.84	0.058	**411**	796.16	463.48	0.024
108	556.63	1626.92	0.058	**412**	796.48	247.67	-0.416
109	556.65	1624.04	0.058	**413**	796.54	531.72	0.067
110	556.68	1619.06	0.058	**414**	796.80	389.17	-0.033
111	556.69	1617.68	0.058	**415**	796.98	530.70	0.066
112	556.73	1612.55	0.058	**416**	797.20	388.07	-0.034
113	556.73	1611.24	0.058	**417**	797.24	371.33	-0.049
114	556.75	1608.47	0.058	**418**	797.30	529.66	0.066
115	556.79	1603.34	0.058	**419**	797.65	528.64	0.065
116	556.83	1597.40	0.057	**420**	797.71	246.62	-0.432
117	556.85	1593.42	0.057	**421**	797.76	462.14	0.024
118	556.86	1591.85	0.057	**422**	797.81	370.32	-0.050
119	556.91	1587.62	0.057	**423**	798.33	527.64	0.065
120	557.00	1583.61	0.057	**424**	798.40	369.29	-0.051
121	557.16	1576.95	0.057	**425**	798.54	526.61	0.064
122	557.27	1572.47	0.057	**426**	798.72	460.91	0.023
123	557.37	1566.94	0.055	**427**	798.76	574.04	0.087
124	557.48	1548.74	0.055	**428**	798.97	575.32	0.088
125	557.66	1542.04	0.055	**429**	799.02	368.20	-0.052
126	557.88	1534.30	0.055	**430**	799.15	525.59	0.064
127	558.03	1528.74	0.055	**431**	799.25	459.26	0.021
128	558.23	1521.34	0.055	**432**	799.27	385.78	-0.036
129	558.71	1504.13	0.055	**433**	799.57	480.30	0.036
130	558.76	1502.32	0.055	**434**	799.68	524.58	0.063
131	559.45	769.28	0.054	**435**	799.87	366.69	-0.054
132	559.49	768.28	0.054	**436**	800.12	523.56	0.062
133	559.65	763.62	0.052	**437**	800.13	386.81	-0.035
134	559.69	762.58	0.052	**438**	800.40	384.72	-0.037
135	559.73	761.31	0.051	**439**	800.56	522.53	0.062
136	559.80	759.37	0.051	**440**	800.73	479.26	0.035
137	560.09	750.79	0.048	**441**	800.77	365.12	-0.055
138	560.13	749.69	0.047	**442**	801.35	332.28	-0.090
139	560.24	746.53	0.046	**443**	801.37	364.06	-0.056
140	560.29	745.10	0.045	**444**	801.60	519.65	0.060
141	560.55	737.51	0.042	**445**	801.77	516.07	0.058
142	560.74	735.73	0.042	**446**	801.94	363.06	-0.057
143	561.07	734.37	0.042	**447**	801.99	331.14	-0.091
144	561.41	733.06	0.048	**448**	802.24	245.40	-0.395
145	561.46	731.61	0.048	**449**	802.29	382.75	-0.039
146	561.77	722.73	0.044	**450**	802.40	362.05	-0.058
147	562.14	715.77	0.042	**451**	802.57	360.94	-0.059
148	562.44	714.55	0.042	**452**	802.73	359.88	-0.060
149	562.72	713.55	0.041	**453**	802.89	358.88	-0.061
150	563.00	712.51	0.041	**454**	802.95	512.22	0.056
151	563.26	711.48	0.048	**455**	803.04	357.85	-0.062
152	563.72	697.98	0.043	**456**	803.10	329.94	-0.092
153	564.08	694.47	0.042	**457**	803.16	381.54	-0.040
154	564.38	693.37	0.041	**458**	803.19	569.07	0.085
155	564.67	692.30	0.041	**459**	803.21	356.75	-0.063
156	564.95	691.27	0.041	**460**	803.45	511.04	0.055

157	571.85	665.80	0.032	**461**	803.48	244.34	-0.403
158	572.13	664.76	0.031	**462**	803.94	570.20	0.086
159	577.10	646.47	0.025	**463**	803.99	509.76	0.055
160	577.85	643.86	0.024	**464**	804.09	380.54	-0.041
161	581.69	630.61	0.019	**465**	804.52	508.51	0.054
162	582.09	629.23	0.019	**466**	804.66	243.33	-0.412
163	586.39	614.37	0.013	**467**	804.67	328.53	-0.094
164	586.68	613.36	0.013	**468**	804.94	507.50	0.053
165	587.68	609.89	0.012	**469**	805.22	379.30	-0.042
166	587.98	608.86	0.011	**470**	805.42	506.37	0.053
167	589.95	602.06	0.009	**471**	805.86	327.46	-0.096
168	590.27	600.94	0.008	**472**	805.88	505.28	0.052
169	590.60	599.82	0.008	**473**	805.88	242.29	-0.421
170	595.35	583.39	0.002	**474**	806.26	378.16	-0.043
171	595.72	582.11	0.002	**475**	806.34	504.19	0.051
172	596.12	580.74	0.001	**476**	806.83	503.01	0.050
173	597.41	576.50	-0.001	**477**	807.16	326.30	-0.097
174	597.83	575.32	-0.001	**478**	807.24	241.25	-0.443
175	598.25	574.04	-0.019	**479**	807.27	501.96	0.050
176	599.31	570.20	-0.020	**480**	807.33	377.00	-0.044
177	599.64	569.07	-0.020	**481**	807.71	500.93	0.049
178	605.56	548.63	-0.028	**482**	808.29	325.29	-0.099
179	605.95	547.27	-0.028	**483**	808.47	375.76	-0.045
180	606.29	546.08	-0.029	**484**	808.62	498.76	0.048
181	606.92	543.91	-0.030	**485**	809.15	497.51	0.047
182	609.87	533.95	-0.034	**486**	809.51	324.20	-0.100
183	610.29	532.77	-0.034	**487**	809.63	374.68	-0.046
184	610.67	531.72	-0.035	**488**	810.44	580.74	0.090
185	611.03	530.70	-0.035	**489**	810.44	340.17	-0.080
186	611.40	529.66	-0.036	**490**	810.50	373.66	-0.047
187	611.76	528.64	-0.037	**491**	810.70	323.13	-0.101
188	612.12	527.64	-0.037	**492**	810.76	495.08	0.046
189	612.49	526.61	-0.038	**493**	811.07	339.08	-0.081
190	612.86	525.59	-0.038	**494**	811.22	582.11	0.091
191	613.21	524.58	-0.039	**495**	811.56	583.39	0.091
192	613.58	523.56	-0.040	**496**	811.59	338.01	-0.082
193	613.95	522.53	-0.040	**497**	811.99	321.98	-0.103
194	614.97	519.65	-0.042	**498**	812.51	240.25	-0.412
195	616.17	516.07	-0.032	**499**	812.95	336.61	-0.084
196	617.36	512.22	-0.033	**500**	813.21	320.89	-0.104
197	617.78	511.04	-0.033	**501**	813.94	239.12	-0.428
198	618.24	509.76	-0.034	**502**	814.18	335.51	-0.085
199	618.68	508.51	-0.035	**503**	814.36	319.86	-0.106
200	619.04	507.50	-0.036	**504**	814.85	608.86	0.102
201	619.45	506.37	-0.036	**505**	815.38	334.44	-0.087
202	619.84	505.28	-0.037	**506**	815.58	318.76	-0.107
203	620.23	504.19	-0.037	**507**	815.76	576.50	0.088
204	620.65	503.01	-0.038	**508**	816.56	333.38	-0.088
205	621.02	501.96	-0.039	**509**	816.63	238.09	-0.444
206	621.39	500.93	-0.039	**510**	816.73	317.73	-0.109
207	622.17	498.76	-0.041	**511**	818.69	315.98	-0.111
208	622.61	497.51	-0.041	**512**	819.82	314.97	-0.112
209	623.48	495.08	-0.043	**513**	820.95	485.75	0.040

210	626.82	485.75	-0.048	**514**	821.04	313.88	-0.114
211	627.26	484.58	-0.049	**515**	821.54	484.58	0.039
212	628.86	480.30	-0.051	**516**	822.15	312.88	-0.115
213	629.24	479.26	-0.052	**517**	822.18	236.69	-0.451
214	634.67	464.71	-0.060	**518**	823.34	311.82	-0.117
215	635.13	463.48	-0.061	**519**	823.61	235.58	-0.419
216	635.63	462.14	-0.061	**520**	824.54	310.74	-0.118
217	636.09	460.91	-0.062	**521**	824.91	234.49	-0.441
218	636.71	459.26	-0.063	**522**	825.67	309.73	-0.120
219	638.44	454.62	-0.066	**523**	826.82	233.47	-0.455
220	638.92	453.33	-0.066	**524**	826.83	308.70	-0.121
221	639.38	452.23	-0.067	**525**	827.86	307.69	-0.122
222	639.95	450.94	-0.068	**526**	828.37	232.46	-0.457
223	640.44	449.84	-0.068	**527**	828.78	295.37	-0.141
224	640.97	448.61	-0.069	**528**	828.99	306.52	-0.124
225	641.52	447.38	-0.070	**529**	829.68	600.94	0.099
226	641.98	446.33	-0.070	**530**	829.91	294.21	-0.143
227	642.93	443.92	-0.059	**531**	830.02	305.46	-0.126
228	644.59	439.48	-0.062	**532**	830.74	599.82	0.099
229	645.00	438.39	-0.063	**533**	831.02	293.06	-0.145
230	645.38	437.36	-0.063	**534**	831.03	304.40	-0.127
231	645.79	436.26	-0.064	**535**	832.09	303.31	-0.129
232	646.47	434.45	-0.065	**536**	832.83	289.20	-0.150
233	646.90	433.41	-0.065	**537**	833.11	302.26	-0.131
234	647.38	432.33	-0.066	**538**	833.31	288.19	-0.152
235	648.04	430.82	-0.067	**539**	833.36	231.46	-0.454
236	648.57	429.62	-0.068	**540**	833.96	602.06	0.100
237	650.70	424.77	-0.070	**541**	834.53	300.79	-0.133
238	651.18	423.68	-0.071	**542**	834.86	230.45	-0.456
239	652.05	421.77	-0.072	**543**	835.12	287.06	-0.154
240	652.66	420.70	-0.073	**544**	835.59	299.69	-0.135
241	653.24	419.67	-0.074	**545**	836.09	273.98	-0.174
242	654.05	418.25	-0.075	**546**	836.22	263.20	-0.190
243	654.67	417.15	-0.076	**547**	836.41	229.44	-0.458
244	657.13	411.15	-0.112	**548**	836.59	298.66	-0.136
245	657.64	410.11	-0.112	**549**	836.67	262.12	-0.192
246	658.20	409.00	-0.100	**550**	837.65	297.57	-0.138
247	658.92	407.07	-0.101	**551**	837.77	260.99	-0.194
248	659.64	405.14	-0.102	**552**	837.78	258.14	-0.199
249	660.12	403.84	-0.103	**553**	837.88	272.84	-0.175
250	660.58	402.61	-0.104	**554**	838.49	271.60	-0.177
251	661.06	401.34	-0.104	**555**	838.60	269.41	-0.181
252	661.72	399.55	-0.105	**556**	838.68	296.50	-0.139
253	662.15	398.41	-0.106	**557**	838.76	283.29	-0.159
254	663.97	393.53	-0.109	**558**	839.49	270.47	-0.179
255	664.36	392.50	-0.110	**559**	839.78	282.23	-0.161
256	665.35	390.64	-0.111	**560**	840.42	259.89	-0.196
257	666.36	389.17	-0.112	**561**	842.02	228.44	-0.462
258	667.12	388.07	-0.113	**562**	843.37	265.74	-0.186
259	667.98	386.81	-0.114	**563**	843.52	256.26	-0.203
260	668.69	385.78	-0.114	**564**	844.76	226.55	-0.465
261	669.42	384.72	-0.115	**565**	845.19	264.70	-0.188
262	670.77	382.75	-0.117	**566**	846.35	225.50	-0.467

263	671.60	381.54	-0.118	**567**	848.54	224.49	-0.469
264	672.28	380.54	-0.109	**568**	850.28	253.07	-0.210
265	672.74	379.30	-0.109	**569**	850.66	255.19	-0.206
266	673.16	378.16	-0.110	**570**	853.96	251.96	-0.213
267	673.77	377.00	-0.110	**571**	853.99	223.46	-0.469
268	674.60	375.76	-0.111	**572**	855.26	254.19	-0.208
269	675.34	374.68	-0.112	**573**	859.22	221.95	-0.498
270	676.04	373.66	-0.112	**574**	861.49	220.94	-0.475
271	676.82	372.53	-0.113	**575**	862.26	250.86	-0.216
272	677.64	371.33	-0.114	**576**	864.62	219.09	-0.479
273	678.34	370.32	-0.115	**577**	865.77	246.62	-0.228
274	679.04	369.29	-0.116	**578**	865.82	249.84	-0.218
275	679.79	368.20	-0.116	**579**	866.94	217.85	-0.491
276	680.83	366.69	-0.118	**580**	868.07	217.85	-0.475
277	681.93	365.12	-0.119	**581**	872.17	245.40	-0.231
278	682.66	364.06	-0.121	**582**	873.38	219.09	-0.447
279	683.35	363.06	-0.122	**583**	873.69	226.55	-0.356
280	684.06	362.05	-0.127	**584**	873.97	248.79	-0.221
281	684.83	360.94	-0.131	**585**	874.84	247.67	-0.223
282	685.56	359.88	-0.136	**586**	875.24	225.50	-0.364
283	686.26	358.88	-0.141	**587**	877.46	243.33	-0.240
284	686.97	357.85	-0.146	**588**	877.54	244.34	-0.234
285	687.76	356.75	-0.150	**589**	878.28	224.49	-0.372
286	691.40	352.00	-0.154	**590**	879.37	240.25	-0.254
287	692.18	350.98	-0.155	**591**	879.52	216.71	-0.587
288	693.15	349.71	-0.156	**592**	880.59	241.25	-0.248
289	693.92	348.71	-0.157	**593**	882.11	221.95	-0.404
290	694.93	347.39	-0.159	**594**	882.27	223.46	-0.384
291	700.49	340.17	-0.175	**595**	882.28	242.29	-0.243
292	701.33	339.08	-0.176	**596**	885.49	220.94	-0.418
293	702.15	338.01	-0.177	**597**	885.63	228.44	-0.337
294	703.22	336.61	-0.179	**598**	886.12	239.12	-0.262
295	704.06	335.51	-0.180	**599**	887.58	216.71	-0.559
296	704.89	334.44	-0.181	**600**	888.45	238.09	-0.268
297	705.69	333.38	-0.182	**601**	888.69	236.69	-0.278
298	706.54	332.28	-0.183	**602**	888.77	235.58	-0.286
299	707.45	331.14	-0.182	**603**	889.71	229.44	-0.329
300	708.33	329.94	-0.185	**604**	890.36	234.49	-0.293
301	709.49	328.53	-0.186	**605**	892.61	233.47	-0.300
302	710.47	327.46	-0.187	**606**	892.96	232.46	-0.307
303	711.53	326.30	-0.187	**607**	893.39	230.45	-0.322
304	548.59	5718.71	0.062				

Appendix III: Energy Consumption of Synthetic Smart Grid Buildings for *FII*

Building Number	H 1	H 2	H 3	H 4	H 5	H 6	H7	H 8	H 9	H 10
B 1	1.13	1.14	1.13	0.96	0.83	0.95	1.00	1.43	1.24	1.54
B 2	1.30	1.12	1.12	0.95	0.97	1.16	1.34	1.64	1.38	1.64
B 3	0.62	0.69	0.82	0.63	0.79	0.76	0.94	0.69	0.95	0.93
B 4	1.13	1.06	0.87	1.10	1.04	1.02	1.15	1.16	1.12	1.44
B 5	1.02	0.94	0.93	0.86	0.85	1.26	1.27	1.17	1.13	1.28
B 6	0.81	0.82	0.85	0.87	0.72	0.95	0.98	0.95	1.07	1.16
B 7	1.00	0.84	0.87	0.86	0.84	1.09	0.92	1.00	1.11	1.15
B 8	1.09	0.88	0.87	0.87	0.91	0.97	1.10	0.79	1.24	1.58
B 9	1.33	1.29	1.52	0.95	1.54	1.36	1.58	1.25	1.60	1.80
B 10	1.30	1.23	1.29	1.23	1.23	1.40	1.48	1.44	1.49	1.62
B 11	0.91	0.90	0.87	0.73	0.84	0.85	0.99	1.00	1.18	1.16
B 12	1.20	1.24	0.95	1.32	1.13	1.11	1.34	1.23	1.63	1.67
B 13	1.18	1.08	0.92	0.80	1.18	0.98	1.15	1.25	1.36	1.33
B 14	1.04	0.88	0.90	0.93	0.75	1.07	1.31	1.20	1.21	1.41
B 15	1.07	1.11	1.02	1.02	0.85	0.94	1.08	1.19	1.49	1.42
B 16	1.00	0.95	0.97	0.90	1.07	0.98	1.22	1.00	1.29	1.30
B 17	1.00	1.12	0.88	0.95	0.91	0.77	0.94	1.15	1.23	1.19
B 18	1.12	1.21	1.15	1.05	1.13	1.16	1.10	1.36	1.34	1.47
B 19	1.36	1.04	0.98	0.85	1.16	1.20	1.20	1.37	1.46	1.60
B 20	1.36	1.25	0.92	0.79	1.16	0.91	1.22	1.26	1.75	1.54
B 21	1.19	1.00	1.09	1.03	0.97	0.95	1.01	1.14	1.28	1.39
B 22	0.86	0.91	0.93	0.67	0.90	0.98	0.93	1.14	1.12	1.05
B 23	1.01	0.97	1.08	0.98	1.03	1.13	1.15	1.25	1.43	1.63
B 24	1.02	1.16	1.17	1.08	1.18	1.36	1.34	1.32	1.55	1.65
B 25	0.84	0.90	0.88	0.84	0.81	1.05	0.93	1.17	1.42	1.43
B 26	1.06	0.93	0.96	1.03	1.04	1.00	1.26	1.29	1.47	1.44
B 27	1.07	1.09	0.90	1.00	1.00	1.18	1.11	1.17	1.19	1.26
B 28	0.84	0.95	0.86	0.85	0.78	1.02	1.07	1.06	1.34	1.20
B 29	0.93	0.86	0.86	0.91	0.92	1.19	1.03	1.11	1.09	1.33
B 30	0.81	0.72	0.89	0.87	0.86	0.94	1.08	1.11	1.09	1.35
B 31	1.00	0.92	1.06	1.26	1.08	0.98	1.25	1.06	1.17	1.59
B 32	0.94	0.83	0.77	0.76	0.89	0.70	0.92	1.00	1.04	1.26
B 33	0.99	0.85	0.85	0.86	0.82	0.91	0.83	1.09	1.01	0.99
B 34	0.81	0.70	0.80	0.85	0.93	0.90	0.86	1.04	1.02	1.13
B 35	0.90	0.75	0.67	0.58	0.58	0.72	0.86	0.65	0.84	0.95
B 36	1.17	1.24	1.07	0.93	0.97	1.09	1.19	1.15	1.46	1.75
B 37	4.93	3.62	4.13	3.56	3.02	3.65	5.89	6.60	8.58	12.01
B 38	4.51	4.21	3.55	3.52	3.56	4.65	4.67	8.99	11.42	12.09

B 39	5.61	4.97	4.46	4.23	5.02	4.41	5.02	9.73	11.82	12.50
B 40	6.69	4.93	5.49	4.40	4.11	4.80	7.25	8.70	11.49	16.28
B 41	4.63	4.38	3.92	4.09	4.30	3.57	5.56	6.46	11.63	14.09
B 42	5.44	6.07	4.29	4.12	4.30	5.19	6.47	9.35	12.57	13.35
B 43	5.80	4.47	5.20	3.93	3.54	3.97	5.35	7.23	11.28	15.16
B 44	6.22	6.01	5.77	3.85	3.58	4.23	6.58	8.53	14.02	12.71
B 45	5.06	4.28	4.49	3.26	3.20	4.54	6.09	7.82	10.42	11.22
B 46	5.08	5.06	4.41	4.09	3.90	5.08	6.23	9.55	8.92	12.82
B 47	64.8	50.7	59.2	43.2	44.4	49.0	73.2	95.8	130.1	202.9
B 48	68.6	57.1	54.8	44.0	42.8	54.2	69.8	94.5	135.1	153.3
B 49	65.6	69.9	63.1	66.4	49.9	46.2	91.8	121.9	138.7	180.7
B 50	77.1	67.8	62.2	46.3	44.4	60.2	75.9	122.1	167.3	166.7

Building Number	**H 11**	**H 12**	**H 13**	**H 14**	**H 15**	**H 16**	**H 17**	**H 18**	**H 19**	**H 20**
B 1	1.58	2.06	1.85	1.80	1.87	2.32	2.24	2.16	2.39	2.08
B 2	1.80	1.71	2.15	1.93	2.66	2.26	2.58	2.34	2.42	2.14
B 3	1.53	1.50	1.67	1.38	1.53	1.58	1.86	1.58	1.65	1.18
B 4	1.53	1.76	1.83	2.04	1.80	2.49	2.47	2.27	2.15	1.92
B 5	1.55	2.00	1.70	1.57	1.83	2.23	2.32	2.26	2.02	2.02
B 6	1.29	1.56	1.66	1.87	2.08	1.91	1.84	1.93	1.76	1.50
B 7	1.44	1.67	2.10	1.85	1.77	2.33	2.32	1.96	1.61	1.76
B 8	1.42	2.03	2.03	2.05	2.18	1.83	2.21	2.51	2.08	2.00
B 9	2.17	2.03	2.70	2.37	2.83	3.03	3.03	3.15	2.97	2.44
B 10	2.19	1.92	2.42	2.04	2.92	2.91	2.76	2.66	1.91	2.60
B 11	1.31	1.71	1.29	1.63	1.57	1.74	1.99	1.96	1.54	1.58
B 12	2.43	2.60	1.86	2.70	2.32	2.66	2.86	2.93	2.52	2.90
B 13	1.57	1.90	2.34	1.95	2.40	2.32	2.26	2.01	2.07	2.04
B 14	1.37	2.12	2.07	2.13	1.88	2.15	2.03	2.02	1.86	1.71
B 15	1.85	2.01	2.28	2.16	2.08	1.91	2.35	2.43	2.07	1.95
B 16	1.59	1.86	1.45	1.69	1.74	2.13	2.43	1.98	2.10	1.99
B 17	1.42	1.81	1.69	2.15	1.92	2.44	1.90	2.11	1.66	1.76
B 18	1.79	2.00	2.15	2.42	2.63	2.36	2.56	2.35	2.34	2.31
B 19	1.77	2.13	2.19	2.90	2.09	1.95	2.18	2.13	2.17	2.16
B 20	1.66	2.09	2.22	2.28	2.22	2.10	2.54	2.07	2.03	2.49
B 21	1.80	1.86	2.26	2.01	2.43	2.12	2.35	2.45	2.03	1.96
B 22	1.05	1.52	1.79	1.80	1.90	1.74	1.93	1.54	1.61	1.55
B 23	1.72	2.19	2.04	2.12	2.60	2.13	2.31	2.45	2.16	2.35
B 24	1.55	2.00	2.48	2.30	2.55	2.19	2.53	2.58	2.00	2.31
B 25	1.62	1.81	1.70	2.07	2.38	2.58	2.17	1.84	2.12	2.09
B 26	1.87	2.11	2.62	2.43	2.55	2.32	2.08	2.23	2.03	2.00
B 27	1.70	1.87	2.14	1.94	2.65	2.27	2.56	2.20	2.10	2.20
B 28	1.55	1.80	1.91	1.79	2.08	1.93	1.91	1.79	2.13	1.71
B 29	1.37	1.85	2.12	2.13	1.98	1.80	2.55	2.60	2.07	1.78
B 30	1.44	1.57	1.54	1.95	1.84	1.94	1.83	1.63	1.86	1.76

B 31	1.54	2.01	2.36	2.25	2.47	1.91	2.51	2.77	2.28	1.77
B 32	1.35	1.44	1.71	1.71	1.76	1.72	1.92	1.51	1.69	1.61
B 33	1.56	1.59	1.77	1.71	1.66	1.30	2.05	1.82	1.74	1.79
B 34	1.32	1.44	1.70	1.66	1.85	1.84	1.90	1.83	2.05	1.87
B 35	0.87	1.37	1.29	1.67	1.41	1.54	1.35	1.39	1.24	1.41
B 36	1.71	2.01	1.70	2.10	2.04	2.30	2.60	2.76	2.68	2.17
B 37	15.69	13.09	12.12	11.83	15.25	12.56	12.38	8.86	8.86	7.46
B 38	12.81	12.29	12.88	12.29	12.60	13.66	12.41	10.80	8.67	6.97
B 39	18.74	15.67	13.76	13.70	13.27	11.62	12.80	9.97	9.89	7.91
B 40	16.42	17.76	14.89	17.61	12.75	17.04	18.29	14.19	11.69	9.20
B 41	11.44	16.39	11.01	14.03	15.23	13.23	15.18	13.12	8.69	6.11
B 42	16.08	14.96	12.63	16.40	15.52	14.37	14.28	12.70	10.01	8.64
B 43	15.30	15.77	14.83	10.90	14.29	14.29	14.01	9.48	8.17	8.62
B 44	13.65	16.87	16.65	15.20	14.43	15.47	12.44	12.42	11.18	9.29
B 45	14.23	12.15	12.61	13.62	14.76	12.05	12.68	10.72	7.53	7.40
B 46	15.27	13.67	11.71	15.83	15.83	14.58	13.95	10.21	8.86	8.11
B 47	163.1	173.2	198.7	154.1	183.7	147.6	172.8	134.8	115.9	93.09
B 48	213.3	169.5	200.1	181.0	160.8	167.6	185.1	156.0	119.4	106.4
B 49	211.6	203.9	189.0	194.1	195.6	188.2	162.7	168.2	122.8	115.4
B 50	213.8	224.1	182.6	228.5	217.5	190.8	192.5	150.3	117.8	112.0

Building Number	**H 21**	**H 22**	**H 23**	**H 24**
B 1	1.95	1.90	1.30	1.41
B 2	2.25	1.98	1.86	1.45
B 3	1.35	1.10	0.87	1.02
B 4	2.17	1.67	1.35	1.54
B 5	1.78	1.74	1.19	1.35
B 6	1.73	1.39	1.18	1.14
B 7	1.71	1.53	1.25	1.25
B 8	1.74	1.60	1.42	1.35
B 9	2.53	1.91	1.58	1.86
B 10	1.81	1.53	1.72	1.45
B 11	1.59	1.31	1.19	1.13
B 12	2.25	2.09	1.86	1.65
B 13	1.66	1.70	1.32	1.33
B 14	1.64	1.51	1.10	1.32
B 15	1.88	1.48	1.36	1.32
B 16	1.59	1.58	1.21	1.41
B 17	1.69	1.60	1.45	1.27
B 18	1.96	1.84	1.63	1.45
B 19	2.02	1.87	1.59	1.54
B 20	1.98	1.75	1.67	1.39
B 21	2.32	1.82	1.37	1.42
B 22	1.68	1.37	1.04	1.10

B 23	2.15	1.71	1.32	1.42
B 24	2.07	1.64	1.55	1.18
B 25	1.86	1.44	1.69	1.00
B 26	2.11	1.62	1.35	1.33
B 27	2.05	1.48	1.22	1.20
B 28	1.73	1.33	1.26	0.82
B 29	2.09	1.51	1.31	1.40
B 30	1.87	1.55	1.36	1.07
B 31	1.94	1.61	1.51	1.42
B 32	1.46	1.47	1.10	1.17
B 33	1.39	1.29	1.33	1.19
B 34	1.68	1.22	1.03	0.92
B 35	1.45	1.03	0.99	0.84
B 36	2.01	1.92	1.61	1.54
B 37	5.78	5.90	4.99	4.95
B 38	6.27	6.42	4.93	5.54
B 39	8.74	7.69	6.04	5.41
B 40	8.73	7.90	6.92	5.89
B 41	6.61	5.65	5.07	4.57
B 42	7.92	6.97	5.69	6.24
B 43	7.18	6.90	5.25	4.56
B 44	6.69	7.04	6.41	7.32
B 45	7.68	6.03	5.13	5.19
B 46	6.94	6.93	7.38	5.32
B 47	89.19	89.89	53.80	54.63
B 48	100.02	72.31	70.88	57.64
B 49	89.80	78.87	77.84	71.78
B 50	1.95	1.90	1.30	1.41